ESC European Society of Cardiology

Cardiovascular Research (2023) **119**, 236–251
https://doi.org/10.1093/cvr/cvac012

Rapid neutrophil mobilization by VCAM-1+ endothelial cell-derived extracellular vesicles

Naveed Akbar [1], Adam T. Braithwaite [1], Emma M. Corr[2], Graeme J. Koelwyn[2], Coen van Solingen [2], Clément Cochain [3], Antoine-Emmanuel Saliba[4], Alastair Corbin [5], Daniela Pezzolla [1], Malene Møller Jørgensen [6,7], Rikke Bæk [7], Laurienne Edgar [1], Carla De Villiers[8], Mala Gunadasa-Rohling [8], Abhirup Banerjee [1], Daan Paget [1], Charlotte Lee [1], Eleanor Hogg [1], Adam Costin [9], Raman Dhaliwal [9], Errin Johnson[9], Thomas Krausgruber [10], Joey Riepsaame [9], Genevieve E. Melling[11,12], Mayooran Shanmuganathan[1,13,14], Oxford Acute Myocardial Infarction Study (OxAMI), Christoph Bock [10,15], David R.F. Carter[11], Keith M. Channon[1,13,14], Paul R. Riley [8], Irina A. Udalova[5], Kathryn J. Moore [2], Daniel C. Anthony [16], and Robin P. Choudhury [1,13,14]*

[1]Division of Cardiovascular Medicine, Radcliffe Department of Medicine University of Oxford Level 6, West Wing John Radcliffe Hospital Headington Oxford OX3 9DU, UK; [2]NYU Cardiovascular Research Center, Department of Medicine, Division of Cardiology, School of Medicine, New York University School of Medicine, 435 E 30th St. New York, NY 10016, USA; [3]Comprehensive Heart Failure Center, University Hospital Wurzburg, Anstalt des öffentlichen Rechts Josef-Schneider-Straße 2 97080 Würzburg, Germany; [4]Helmholtz Institute for RNA-based Infection Research (HIRI), Helmholtz-Center for Infection Research (HZI), Inhoffenstraße 7 38124 Braunschweig, Würzburg, Germany; [5]Kennedy Institute of Rheumatology, University of Oxford, Roosevelt Dr, Headington, Oxford OX3 7FY, UK; [6]Department of Clinical Immunology, Aalborg University Hospital, Urbansgade 32-36, DK-9000, Aalborg, Denmark; [7]Department of Clinical Medicine, Aalborg University, Søndre Skovvej 15, Aalborg, Denmark; [8]Department of Physiology, Anatomy and Genetics, University of Oxford, Sherrington Building Parks Road, OX1 3PT, Oxford, UK; [9]Sir William Dunn School of Pathology, University of Oxford, South Parks Road, Oxford, OX1 3RE, UK; [10]CeMM Research Center for Molecular Medicine of the Austrian Academy of Sciences, Lazarettgasse 14, AKH BT 25.3, Vienna, Austria; [11]Department of Biological and Medical Sciences, Oxford Brookes University, Headington Campus Oxford OX3 0BP, UK; [12]Institute of Clinical Sciences, School of Biomedical Sciences, College of Medical and Dental Sciences, University of Birmingham, Edgbaston, Birmingham, B15 2TT, UK; [13]The OxAMI Study is detailed in the Supplementary Acknowledgments; [14]Acute Vascular Imaging Centre, Radcliffe Department of Medicine, University of Oxford, John Radcliffe Hospital, Headington, Oxford, OX3 9DU, UK; [15]Institute of Artificial Intelligence, Center for Medical Statistics, Informatics, and Intelligent Systems, Medical University of Vienna, Spitalgasse 23, BT88 1090, Vienna, Austria; and [16]Department of Pharmacology, University of Oxford, Mansfield Road, Oxford, OX1 3QT, UK

Received 8 June 2021; editorial decision 18 January 2022; accepted 28 January 2022; online publish-ahead-of-print 4 February 2022

Time for primary review: 28 days

See the editorial comment for this article 'Extracellular vesicles selectively mobilize splenic neutrophils', by R. Panda and P. Kubes, https://doi.org/10.1093/cvr/cvad015.

Aims Acute myocardial infarction rapidly increases blood neutrophils (<2 h). Release from bone marrow, in response to chemokine elevation, has been considered their source, but chemokine levels peak up to 24 h after injury, and *after* neutrophil elevation. This suggests that additional non-chemokine-dependent processes may be involved. Endothelial cell (EC) activation promotes the rapid (<30 min) release of extracellular vesicles (EVs), which have emerged as an important means of cell–cell signalling and are thus a potential mechanism for communicating with remote tissues.

Methods and results Here, we show that injury to the myocardium rapidly mobilizes neutrophils from the spleen to peripheral blood and induces their transcriptional activation prior to arrival at the injured tissue. Time course analysis of plasma-EV composition revealed a rapid and selective increase in EVs bearing VCAM-1. These EVs, which were also enriched for miRNA-126, accumulated preferentially in the spleen where they induced local inflammatory gene and chemokine protein expression, and mobilized splenic-neutrophils to peripheral blood. Using CRISPR/Cas9 genome editing, we generated VCAM-1-deficient EC-EVs and showed that its deletion removed the ability of EC-EVs to provoke

* Corresponding author. Tel: +44 (0)1865 234664, E-mail: robin.choudhury@cardiov.ox.ac.uk

the mobilization of neutrophils. Furthermore, inhibition of miRNA-126 *in vivo* reduced myocardial infarction size in a mouse model.

Conclusions Our findings show a novel EV-dependent mechanism for the rapid mobilization of neutrophils to peripheral blood from a splenic reserve and establish a proof of concept for functional manipulation of EV-communications through genetic alteration of parent cells.

Graphical Abstract

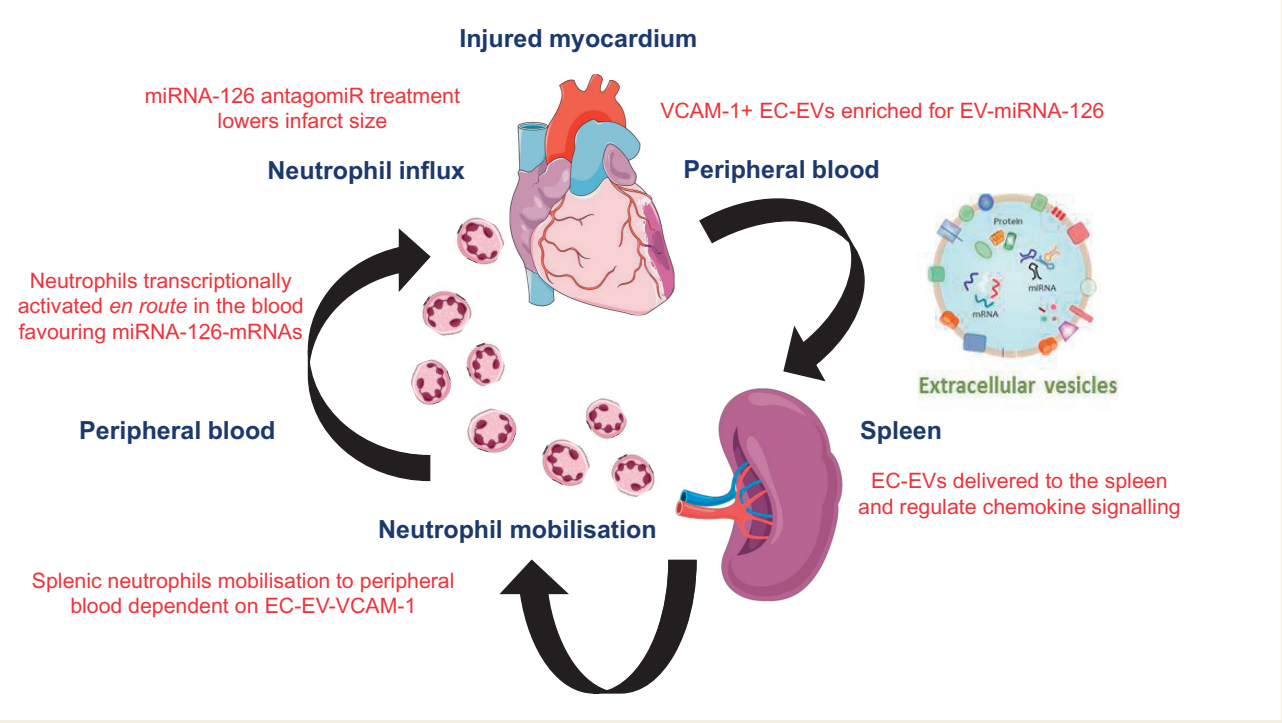

Keywords Exosome • Spleen • Myocardial infarction • Programming

1. Introduction

Acute myocardial infarction (AMI) is a substantial sterile injury that leads to a rapid increase in peripheral blood neutrophils.[1–5] Elevated peripheral blood neutrophil number post-AMI correlates with the extent of myocardial injury, degree of cardiac dysfunction, and mortality.[1–3] Neutrophil depletion enhances susceptibility to cardiac rupture[6] and antibody depletion of neutrophils prior to AMI increases infarct size, enhances fibrosis, and lowers the number of M2 macrophages in the healing myocardium.[1,7] However, inhibition of neutrophil recruitment in AMI reduces infarct size.[1] These competing findings suggest a complex role for neutrophils in the contexts of myocardial ischaemic injury and repair.

The bone marrow is the primary site for granulopoiesis[8,9] and has been regarded as the principal source of neutrophils that are mobilized to peripheral blood after injury.[4,10] Mature neutrophils are held in large numbers in the haemopoietic cords, separated from the blood by the sinusoidal endothelium.[11] In the current paradigm, these cells are retained in the marrow by the interaction of CXCR4 and CXCL12 [stromal cell-derived factor (SDF-1α)][12] and mobilized in response to soluble factors. Intravascular injection of a range of chemotactic factors, including leukotriene B4, C5a, interleukin-8 (IL-8),[13] CXCL chemokines,[12,14] and granulocyte-colony stimulating factor (G-CSF)[15,16] can drive the rapid mobilization of neutrophils across the sinusoidal endothelium. However, numerous strands of evidence question whether chemokines derived from injured tissues are responsible for very early neutrophil mobilization *in vivo*. Intra-cardiac mRNA levels for cytokines peak 12 h after injury[17] and pro-inflammatory proteins are very modestly elevated in coronary sinus following reperfusion therapy in AMI.[18,19] Furthermore, *in vivo* blood chemokine profiles peak 24 h post-AMI and do not precede the rise in blood neutrophil counts in humans or mice, which occurs within 2 h in mice following injury,[1,7] whereas a large majority of rodent AMI studies investigating neutrophils dynamics following AMI have focused on neutrophil elevations 6–24 h post-injury.[1,4] Moreover, a putative source of chemokine generation in the acutely ischaemic myocardium prior to neutrophil infiltration has not been identified.

These observations suggest that neutrophils may be mobilized from alternative reserves following injury and by mechanisms that are not dependent on chemokines. One possible source is extramedullary haematopoiesis in the spleen[20] from where neutrophils are mobilized to

peripheral blood following bacterial infection.[21] By analogy, it is known that monocytes are deployed from a splenic reserve following sterile injury in mice,[22] and that this can be driven by extracellular vesicles (EVs) that are derived from the vascular endothelium.[23]

EVs are membrane-enclosed envelopes[24] that are actively secreted by many cell types.[25–27] These vesicles bear bioactive cargo that includes proteins and microRNAs (miRNAs), which are derived from the parent cell. EV can alter the biological function and cellular status of cells locally[28] and remotely following liberation into the blood.[29] Endothelial cell (EC)-derived EVs (EC-EVs) bearing vascular cell adhesion molecule-1 (VCAM-1) are elevated in the blood following AMI[23,28] and have a role in the mobilization and transcriptional programming of splenic monocytes in AMI.[23]

Here, we sought to establish whether EC-EVs contribute to the very early mobilization and programming of neutrophils and, if so, through which of their component parts. We hypothesized that EC-EVs released during AMI would localize to neutrophils in remote reserves in a process mediated by VCAM-1, which has been shown to bind to neutrophils via surface integrins.[30] Furthermore, we reasoned that once localized to neutrophils in reserve pools, EC-EV-miRNA cargo could induce functionally relevant transcriptional programmes in those target tissues and cells prior to recruitment to the injured myocardium. An understanding of these mechanisms would immediately suggest possibilities for cell-selective immuno-modulatory interventions that are relevant in AMI and, potentially, other pathologies with an inflammatory component.

2. Methods

Translational studies using whole blood, plasma, plasma neutrophils, plasma EV and CMR imaging in human patients, mouse models of AMI with and without antagmiR treatment, RNA-sequencing, flow cytometry, *in vivo* EV injections, and *in vitro* studies using human and mouse ECs were employed here. Full experimental details are provided in the Supplementary material online.

2.1 AMI patients

All clinical investigations were conducted in accordance with the Declaration of Helsinki. The Oxfordshire Research Ethics Committee (references 08/H0603/41 and 11/SC/0397) approved human clinical cohort protocols and conformed to the principles outlined in the Declaration of Helsinki. All patients provided informed written consent for inclusion in the study.

2.2 LAD ligation model

All animal procedures were approved by an ethical review committee at the University of Oxford or NYU Lagone Health. Animal experiments conform to the guidelines from Directive 2010/63/EU of the European Parliament on the protection of animals used for scientific purposes or the current NIH guidelines. UK experimental interventions were carried out by UK Home Office personal licence holders under the authority of a Home Office project licence. AMI was induced in adult wild-type (WT) female C57B6/J mice as previously described.[1] Due to the higher incidence of acute ventricular rupture in male mice.[3] Mice were anesthetized with 4% isofluorane and maintained under 2.5% isoflurane under assisted external ventilation through the insertion of an endotracheal tube (~200 strokes min-1; stroke volume ~200 µL min-1). Buprenorphine (buprenorphine hydrochloride; Vetergesic) was delivered as a 0.015 mg/mL solution via intraperitoneal injection at 20 min before the procedure to provide analgesia. Post-AMI animals were euthanized by cervical dislocation and peripheral blood cells, splenocytes, bone marrow, and cardiac cells were isolated.

2.3 Statistical analysis

All values are group mean ± standard deviation (SD). Paired and unpaired two-tailed Student's *t*-test was used to compare two groups, a one-way or two-way analysis of variance (ANOVA) or mixed model effects with *post-hoc* Bonferroni or Tukey correction was used to compare multiple group (>2) means with one, two or more independent variables. *P*-values <0.05 were considered significant. Hierarchical clustering analysis and generation of heatmap plots was performed using the pheatmap R package v1.0.12.

3. Results

3.1 Plasma neutrophil number correlates with the extent of AMI

In acute ST-segment-elevation AMI (STEMI) peripheral blood neutrophil number at the time of presentation [median time from onset of symptoms to percutaneous coronary intervention (PCI) 3 h] correlated with the extent of ischaemic injury, as determined by oedema estimation on T2-weighted magnetic resonance imaging (MRI) images obtained within 48 h of AMI ($R^2 = 0.365$, $P = 0.017$) (*Figure 1A*) and with final infarct size, determined by late gadolinium enhancement (LGE) MRI 6 months post-AMI ($R^2 = 0.507$, $P = 0.003$) (*Figure 1B*).

3.2 AMI mobilizes neutrophils from the spleen without alterations in systemic chemokines

This rapid increase in peripheral blood neutrophils is consistent with mobilization from an existing reserve. To determine the source of neutrophil mobilization in the very early hours post-AMI, we performed left anterior descending artery ligation in a mouse model of AMI and analysed cell populations from blood, spleen, bone marrow, and the heart 2 h after AMI, by flow cytometry (*Figure 1C*). AMI induced a 6.3-fold ($P < 0.01$) increase in peripheral blood neutrophils (Live, $CD45^+$, $CD11b^+$, $Ly6G^+$) (Supplementary material online, *Figure S1*) and simultaneously lowered splenic-neutrophil number by 0.7-fold ($P < 0.001$) (*Figure 1D*). As described previously, to obtain an indication of the mobilization between reserves, we calculated a neutrophil mobilization ratio[23] [peripheral blood neutrophils/splenic [or bone marrow] neutrophils] and found an increase in splenic-neutrophil mobilization (8.5-fold) ($P < 0.01$), but no alteration in bone marrow neutrophil number relative to control animals. There was no significant alteration in CD62L/L-selectin (which is shed during neutrophil activation) in mobilized peripheral blood neutrophils (*Figure 1E*). At this very early time point (2 h post-AMI), we found no differences in $LyC6^{high}$ monocyte number in the peripheral blood or spleen, indicating that neutrophils mobilize from the spleen prior to splenic-monocyte mobilization[22] (*Figure 1F*).

The prevailing paradigm is that chemokines are rapidly released from ischaemic tissues and mobilize reserves of neutrophils to the peripheral blood following AMI. To determine this in the hyper-acute phase, when splenic-neutrophils are deployed, we undertook a quantitative protein-detection array for 25 different proteins that influence neutrophil function in plasma obtained in 2 h and 24 h post-AMI in our mouse model. We found no alterations in systemic cytokines 2 h post-AMI and only

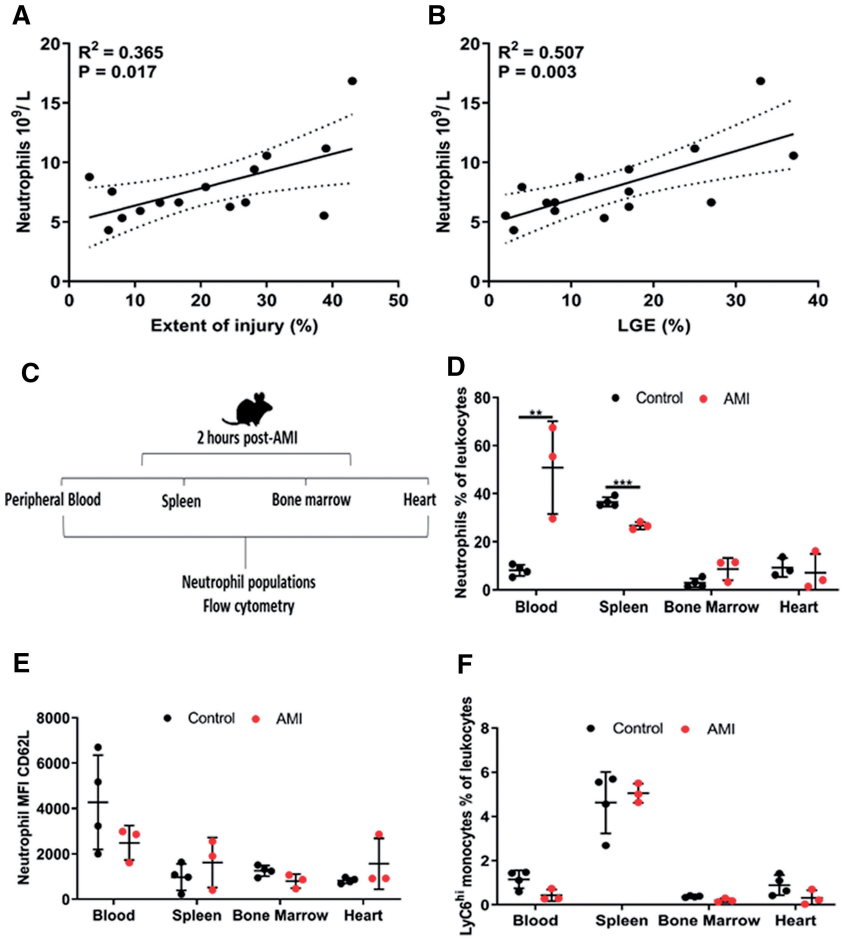

Figure 1 Human peripheral blood neutrophils correlate with the extent of myocardial injury in AMI. (*A*) Pearson's correlation of peripheral blood neutrophil number (10^9/L) in patients experiencing AMI significantly correlated with the extent of myocardial injury (T2-weight MRI) and (*B*) LGE MRI 6-months post-AMI (n=15). (*C*) Schematic representation of mouse AMI and tissue harvesting for flow cytometry. (*D*) Percentage of neutrophils in peripheral blood, spleen, bone marrow, and heart 2 h after AMI in mice relative to the levels of intact controls (controls n = 4, AMI n = 3). (*E*) Mean fluorescence intensity of CD62L/L-selectin on mouse neutrophils in peripheral blood, spleen, bone marrow, and heart 2 h after AMI relative to the levels of intact controls (controls n = 4, AMI n = 3). (*F*) Percentage of monocytes in peripheral blood, spleen, bone marrow, and heart 2 h after AMI in mice relative to the levels of intact uninjured controls (controls n = 4, AMI n=3). Pearson's correlation was used in (*A*) and (*B*), dotted lines represent 95% confidence interval and an unpaired t-test was used in (*D*)–(*F*) for statistical analysis. Error bars represent mean ± SD $^{**}P < 0.01$, $^{***}P < 0.001$.

found a significant increase in CCL6 24 h post-AMI ($P < 0.05$) (Supplementary material online, *Figure S2A*).

S100A8 and S100A9 are released following AMI by activated neutrophils.[4] We measured S100A8/S100A9 heterodimer in the plasma of mice following AMI and found a significant 6.6-fold induction 2 h post-AMI, which was maintained 24 h post-AMI (6.8-fold) when compared to control mice (both, $P < 0.01$) (Supplementary material online, *Figure S1B*). These data demonstrate a rapid increase in peripheral blood neutrophils from the splenic reserve 2 h post-AMI without significant alterations in systemic plasma cytokines.

3.3 Human plasma EVs correlate with the extent of peripheral blood neutrophil counts in AMI and myocardial scar 6-months post-AMI

In agreement with our previous findings, patients with AMI had significantly more plasma EVs at time of presentation ($24.3 \times 10^8 \pm 25.7$ EV/mL) vs. a 6-month follow-up measurement ($11.0 \times 10^8 \pm 12.5$ EV/mL, $P < 0.010$) but they exhibited a similar EV size distribution profile, with an elevation in EVs in the size range 100–200 nm diameter (*Figure 2A and B*). Plasma-EV number at presentation significantly correlated with the extent of myocardial scarring as determined by LGE at 6 months post-AMI ($R^2 = 0.423$, $P = 0.009$) (*Figure 2C*). We also found a highly significant relationship between plasma-EV number and peripheral blood neutrophil number ($R^2 = 0.753$, $P < 0.001$) at time of presentation (*Figure 2D*), consistent with a possible role for plasma EVs in neutrophil mobilization post-AMI.

3.4 Human VCAM-1+ plasma EVs are enriched at time of presentation with AMI

In the same patients, we determined the composition of plasma EVs at six different time points: at presentation (prior to PCI), immediately following PCI and at 6, 24, 48 h, and 6 months post-AMI using a validated high throughput immunoaffinity EV-protein array.[31] To interpret the time course of the EV response after AMI, we normalized the EV-

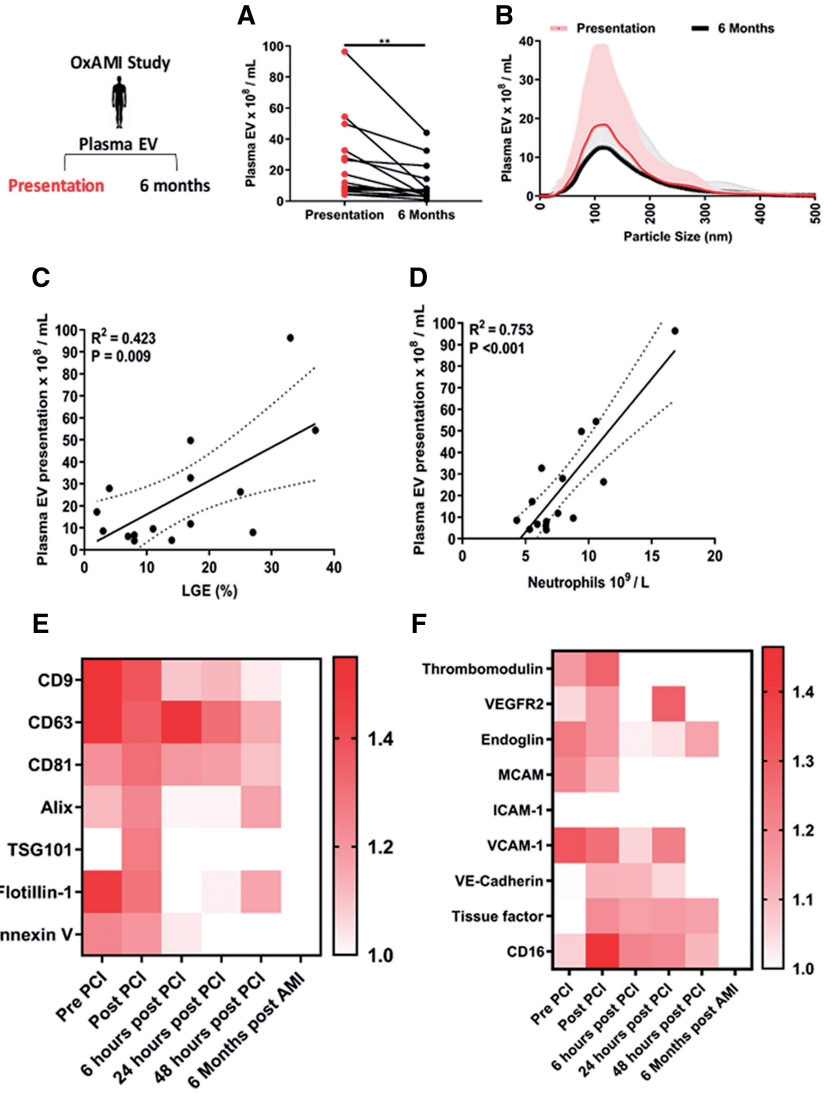

Figure 2 VCAM-1+ plasma EVs are elevated in peripheral blood following AMI. (*A*) Human plasma-EV number (10^8/mL) at time of presentation following AMI and 6 months later in the same patients (n =15). (*B*) Size and concentration profile of human plasma EVs at time of presentation following AMI and 6 months later in the same patients (n =15) determined by Nanoparticle Tracking Analysis. Pearson's correlation of human plasma EVs at time of presentation vs. and: (*C*) LGE MRI 6-months post-AMI, (*D*) number of peripheral blood neutrophils following AMI (10^9/L) (n =15) in the same patients. (*E*) Heat map showing human plasma-EV markers CD9, CD63, CD81, ALIX, TSG101, flotillin-1, annexin V and (*F*) heat map showing human plasma-EV EC markers thrombomodulin, VEGFR2, endoglin, MCAM, ICAM-1, VCAM-1, VE-cadherin, tissue factor and CD16 in the same patients at: presentation, immediately following post-PCI, 6, 24, and 48 h post-PCI and 6 months post-AMI (n = 10 per time point). A paired t-test was used for statistical analysis in (*A*). Error bars in (*B*) represent mean ± SD. Heat maps in (*E*) and (*F*) are group means per time point. Values were normalized to the 6-month time point per patient. Pearson's correlation was used in (*C*) and (*D*), dotted lines represent 95% confidence interval for statistical analysis. $^{**}P < 0.01$.

markers in each patient to those obtained at the 6 months post-AMI time point.

Generic EV-markers CD9, CD63, flotillin-1, CD81, ALIX, and annexin V were highly abundant in plasma EVs at the time of presentation (*Figure 2E*). At presentation plasma-EV number and EV-CD63 (R^2 = 0.863, P = 0.001) and EV-ALIX (R^2 = 0.724, P = 0.018) showed significant associations. Following PCI, there was augmentation of plasma-EV CD81, ALIX, TSG101, and flotillin-1, which subsided 6, 24, and 48 h post-presentation/post-PCI, approaching levels that were comparable to those at 6 months post-AMI (*Figure 2E*). Plasma EVs displayed typical morphology by transmission electron microscopy (TEM) were negative for markers of cellular contamination by histone H3 and washing of plasma EVs with phosphate-buffered saline lowered levels of apoB and albumin in isolated plasma EVs (Supplementary material online, *Figure S3A and B*).

EVs carry proteins on their surface, which can reflect their cellular origin. We determined the composition of EV in relation to EC markers, measuring thrombomodulin, vascular endothelial growth factor receptor 2 (VEGFR2), endoglin, melanoma cell adhesion molecule (MCAM), intercellular adhesion molecule-1 (ICAM-1), VCAM-1, and VE-cadherin on plasma EVs. We additionally examined tissue factor and CD16.

Plasma EVs were enriched for VCAM-1 at the time of presentation, prior to PCI and showed significant associations with plasma-EV number at presentation (R^2 = 0.745, P = 0.013) and with EV-markers CD63 (R^2 = 0.714, P = 0.020) and ALIX (R^2 = 0.651, P = 0.042). VCAM-1+ plasma EV was highest at the earliest time point and diminished over time (*Figure 2F*). Plasma-EV thrombomodulin and VE-cadherin were elevated following PCI but showed no associations with plasma-EV number at presentation. Tissue factor and monocyte/neutrophil marker CD16 also showed distinct patterning post-PCI (*Figure 2F*), but with later peaks than for VCAM-1. These data suggest orchestrated rapid enrichment of plasma EVs-bearing VCAM-1 in the context of AMI.

3.5 Human EC-EVs are enriched for miRNA-126

In order to probe the function of EVs derived exclusively from activated ECs, we studied an established model of primary human umbilical cord vein ECs *in vitro*. Compared with basal conditions, treatment of ECs with pro-inflammatory tumour necrosis factor-α (TNF-α) activated ECs as evidenced by enhanced VCAM-1 protein expression (P < 0.001) (*Figure 3A*) and increased EV production (P < 0.001) (*Figure 3B and C*), with a significant increase in small EVs, of similar size range (100–200 nm) to those found to increase in patients with AMI. EC-EVs displayed typical EV morphology (*Figure 3D and E*), the EV-protein marker CD9 (*Figure 3F*) and were positive for endothelial nitric oxide synthase (eNOS).

EC-EVs derived from pro-inflammatory stimulations show significant enrichment for miRNA-126-3p (P < 0.010) (*Figure 3G*) and miRNA-126-5p (P < 0.010) (*Figure 3H*), consistent with previous observations of changes in miRNA, measured in the unselected plasma-EV pool, following AMI[23] at a time point consistent with elevated VCAM-1+ plasma EVs and prior to PCI.

3.6 miRNA-126-mRNA targets cluster selectively in neutrophil motility pathways

To explore the potential role of EC-EV-miRNA-126, we employed *in silico* techniques, curating miRNA-126 putative-mRNA target genes from three separate miRNA–mRNA target prediction databases for human and mouse.[32–34]

We determined whether the mRNAs putatively regulated by miRNA-126 for the human, mouse or the overlap gene set (targeted in both the human and mouse) (*Figure 3I and J* and Supplementary material online, *Tables S1 and S2*) were present in Gene Ontology (GO) terms for neutrophil function. miRNA-126-putative-mRNA targets were significantly overrepresented when compared by Fisher's exact test to neutrophil pathway GO terms for neutrophil migration (GO: GO1990266) and neutrophil chemotaxis (GO: GO0030593) in the human (both P < 0.001), the mouse (both P < 0.001), and the overlap gene set (both P < 0.001) (Supplementary material online, *Table S3*). Whereas, other neutrophil GO terms, such as neutrophil-mediated killing of a fungus (GO: GO0070947), neutrophil clearance (GO: GO0097350), and regulation of neutrophil-mediated cytotoxicity (GO: 0070948) were not enriched (Supplementary material online, *Table S3*), suggesting a possible role for EC-EV-miRNA-126 in orchestrating processes related to neutrophil mobilization post-AMI.

3.7 AMI alters human and mouse neutrophil transcriptomes

To determine whether neutrophil transcriptomes are altered post-AMI, we obtained peripheral blood neutrophils from newly recruited patients presenting with STEMI (N = 3) and non-STEMI (NSTEMI) control patients (N = 3) at time of presentation and matched-control samples 1 month later. STEMI patients had a greater number of differentially expressed genes at time of presentation vs. NSTEMI control patients (STEMI 933 genes vs. NSTEMI 8 genes) (*Figure 4A–C*).

To further understand the potential target pathways for the differentially enriched genes in blood neutrophils following AMI, we used GO term enrichment analysis and Reactome pathway analysis[35] ranked by false discovery rate (FDR)-adjusted P-values. GO analysis showed that differentially expressed neutrophil genes at the time of presentation favoured pathways for signal recognition particle (SRP)-dependent co-translational protein targeting to membrane (GO: 0006614 and R-HSA-1799339) (both, P < 0.001), co-translational protein targeting to membrane (GO: 0006613) (P < 0.001), and neutrophil degranulation (R-HSA-6798695) (P < 0.001) (Supplementary material online, *Table S4*).

Next, we used single cell (sc)-RNA-sequencing data to determine whether neutrophil populations in the peripheral blood of mice subjected to AMI exhibited similar transcriptomic alterations prior to recruitment to the heart. We found differential enrichment in neutrophil populations in the blood following AMI,[36] which favoured pathway terms for neutrophil aggregation (GO: 0070488) (Supplementary material online, *Tables S5 and S6*) (P < 0.05), platelet activation (GO: 0030168) (P < 0.001), platelet activation, signalling, and aggregation (R-HSA-76002) (P < 0.001) (Supplementary material online, *Table S7*).

There were significant overlaps between the genes that are differentially expressed following AMI in the blood of the human and the mouse (P < 0.001) (Supplementary material online, *Table S8*) and significant similarity in target pathways (GO terms: biological process, molecular function and cellular component, and Reactome pathways) between the human and mouse (Supplementary material online, *Table S9*).

3.8 miRNA-126-mRNA targets are over-represented in neutrophil transcriptomes following AMI

Human miRNA-126-mRNA targets were significantly overrepresented in human neutrophil transcriptomes at the time of injury (P < 0.05) (Supplementary material online, *Table S10*). Similarly, in mice, neutrophils within the myocardium (but not peripheral blood) showed differential enrichment for miRNA-126-mRNA targets (Supplementary material online, *Table S10*).

To test the functional significance of these findings, we treated WT mice with an antagomiR for miRNA-126 (n = 5) or a scramble control (n = 7) prior to induction of experimental AMI. miRNA-126 (*Figure 4D*) reduced infarct size by 12% compared with scramble control (P < 0.01) (*Figure 4E*) (representative images—Supplementary material online, *Figure S4A and B*).

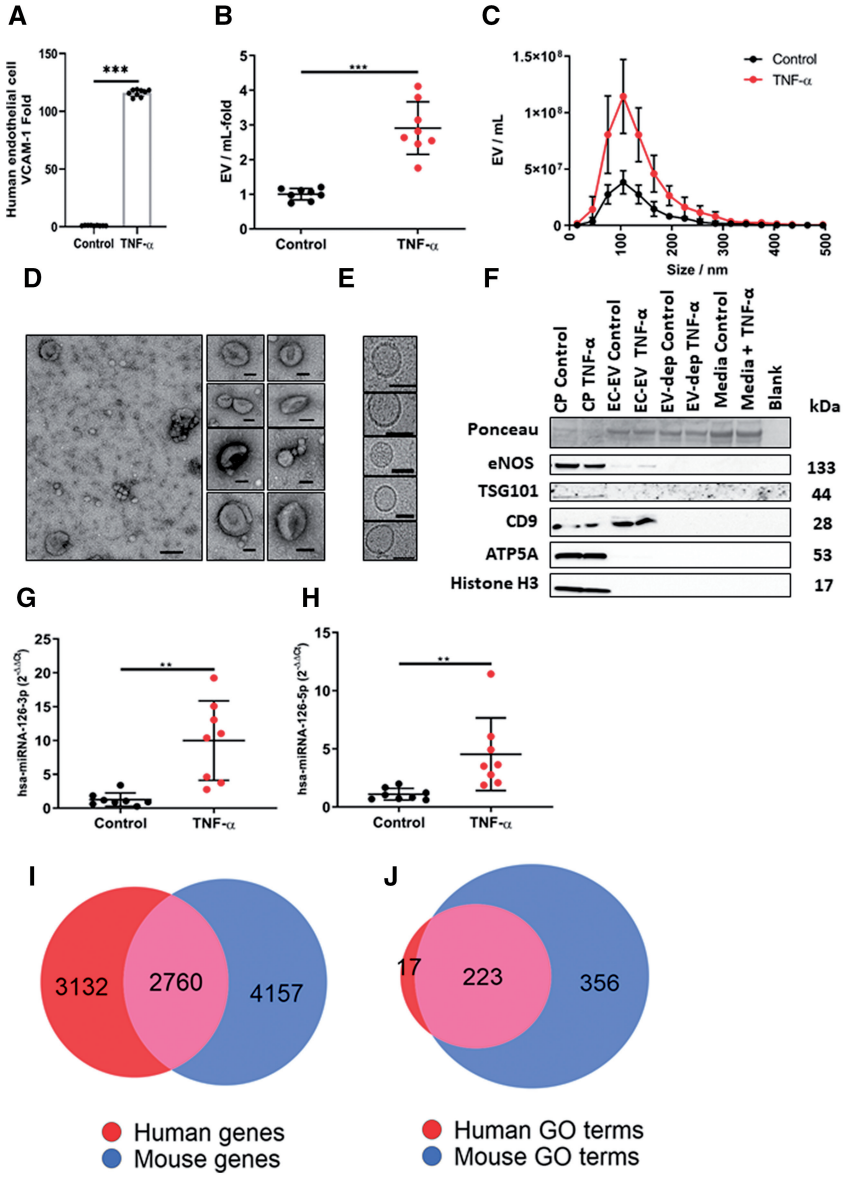

Figure 3 Human umbilical cord vein endothelial cells (HUVEC) release more EVs after inflammatory stimulation. (*A*) HUVECs: express more VCAM-1 following treatment with recombinant human TNF-α (10 ng/mL) ($n = 9$ per group); (*B*) release more EVs ($n = 8$ per group). (*C*) Size and concentration profile of HUVEC-derived EVs under basal conditions and after inflammatory stimulation with recombinant human TNF-α ($n = 8$ per group). (*D*) TEM of HUVEC-derived EVs (scale bar 100 nm) and (*E*) cryo-TEM HUVEC-derived EVs (scale bar 50 nm). (*F*) Ponceau stain and western blot of HUVEC-derived EV from basal and after inflammatory stimulation with TNF-α for eNOS, TSG101, CD9, ATP5A, and Histone H3. HUVEC cell pellets, EV-depleted cell culture supernatants (EV-dep), and cell culture media that was not exposed to cells (control media) were used as controls. EC-EV miRNA levels of (*G*) hsa-miRNA-126-3p and (*H*) hsa-miRNA-126-5p under basal conditions and after inflammatory stimulation with TNF-α ($n = 8$ per group). miRNA-126-mRNA targets in human and mouse and their target pathways. (*I*) Euler plot of miRNA-126-mRNA targets from TargetScanHuman, TargetScanMouse, miRWalk, miRDB for human and the mouse. (*J*) Euler plot of GO terms for miRNA-126-mRNA targets for the human and mouse. Shape areas are approximately proportional to number of genes. An unpaired *t*-test was used in (*A*), (*B*), (*C*), (*G*), and (*H*) for statistical analysis. Error bars represent mean ± SD $^{**}P < 0.01$, $^{***}P < 0.001$.

3.9 EC-EVs localize to the spleen

These accumulating data suggest that EC-EVs, enriched for miRNA-126 and VCAM-1 provide an 'ischaemia signal' to neutrophils in the spleen, resulting in mobilization and transcriptional activation. Accordingly, we tested whether EC-EV localized to the spleen after intravenous injection and whether there were consequent alterations in neutrophil-associated chemokine gene and protein expression. Primary mouse and human ECs release more EVs following inflammatory stimulation[23] and hypoxia.[37] In agreement with these data, mouse sEND.1 ECs produced EV under basal conditions and released significantly more EVs after pro-

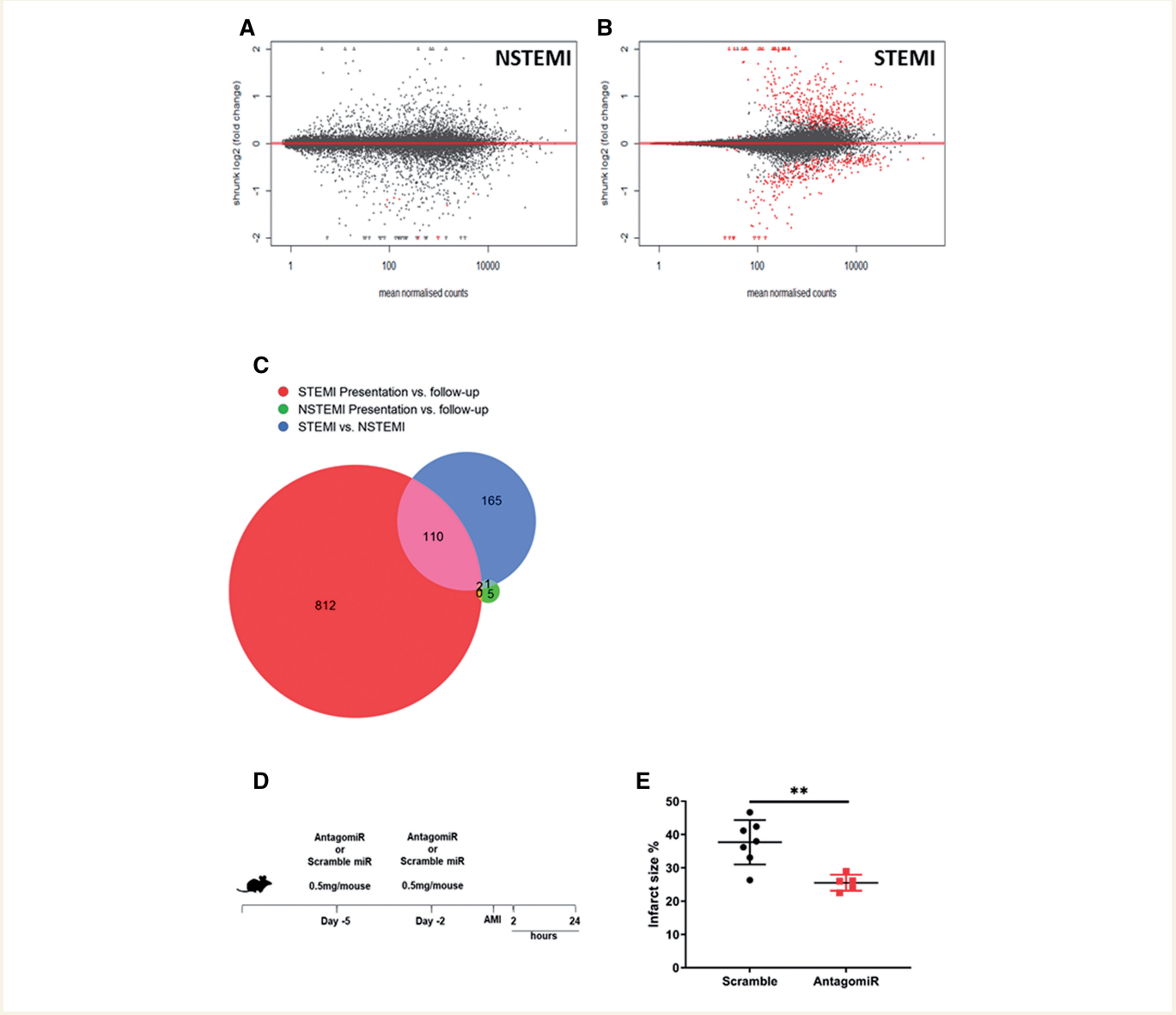

Figure 4 RNA sequencing of human peripheral blood neutrophils. STEMI and NSTEMI patients at the time of presentation vs. a control sample obtained from the same patients 1 month post-AMI (n = 3 per group). MA plots show differential transcriptome at the time of presentation vs. a control sample obtained from the same patients 1 month post-AMI in (*A*) NSTEMI and (*B*) STEMI patients. Significantly altered genes are highlighted in red. (*C*) Euler plot showing similarity and differences in the number of differentially expressed (DE) genes in NSTEMI and STEMI patients at time of presentation vs. 1 month follow-control samples or between all NSTEMI and all STEMI patients (n = 3 per group). (*D*) miRNA-126 antagomiR treatment of WT mice prior to induction of AMI. (*E*) TTC staining of the myocardium 24 h post-AMI in scramble and antagomiR treated mice (scramble n = 7 and antagomiR n = 5 per group). Significant DE genes in (*A*)–(*C*) were determined by adjusted P-values below the 5% FDR threshold. Error bars represent mean ± SD $^{**}P < 0.01$.

inflammatory stimulation with TNF-α ($P < 0.001$) (*Figure 5A and B*).[23] sEND.1 TNF-α-activated ECs produced more VCAM-1 protein ($P < 0.001$) (*Figure 5C*). sEND.1-derived EVs displayed typical EV morphology (*Figure 5D and E*), EV-protein markers (ALIX, TSG101, and CD9) (*Figure 5F*) and were positive for eNOS and VCAM-1. EC-EVs derived from pro-inflammatory stimulations showed significant enrichment for miRNA-126-3p ($P < 0.001$) (*Figure 5G*) and miRNA-126-5p ($P < 0.01$) (*Figure 5H*), indicating similarities in the EC-EV response between human and mouse ECs. We labelled the mouse EC-EV by transfection with non-mammalian miRNA-39, which belongs to *Caenorhabditis elegans* and allows quantitative tracing of EVs *in vivo* (*Figure 6A*). EC-EVs accumulated preferentially in the spleen compared with bone marrow ($P < 0.05$), brain ($P < 0.001$), heart ($P < 0.05$), kidney ($P < 0.05$) (Supplementary material online, *Figure S5A*) 1 h post-injection, and remained detectable in the spleen for 2, 6 ($P < 0.001$), and 24 h ($P < 0.001$) (*Figure 6A*).

3.10 EC-EVs alter chemokine and protein expression in the spleen

Informed by the earlier *in silico* studies suggesting regulation of neutrophil activation and motility by miRNA-126-mRNAs, we hypothesized that

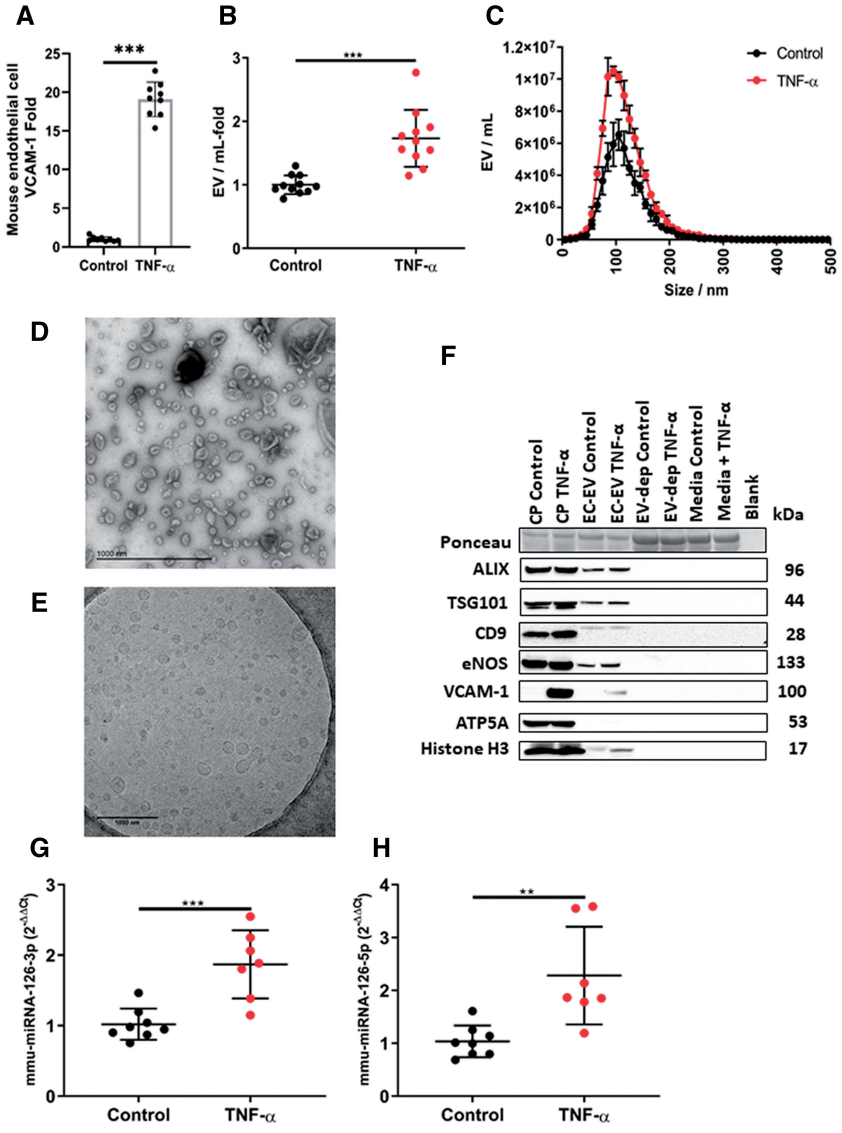

Figure 5 Mouse sEND.1 ECs release more EVs after inflammatory stimulation. (*A*) Mouse sEND.1 ECs express more VCAM-1 following treatment with recombinant mouse TNF-α (10 ng/mL) ($n = 9$ per group); (*B*) release more EVs ($n = 11$ per group). (*C*) Size and concentration profile of sEND.1-derived EVs under basal conditions ($n = 3$) and after inflammatory stimulation with recombinant mouse TNF-α ($n = 4$). (*D*) TEM of sEND.1-derived EVs (scale bar 1000 nm) and (*E*) cryo-TEM sEND.1-derived EVs (scale bar 1000 nm). (*F*) Ponceau stain and western blot of sEND.1-derived EV from basal and after inflammatory stimulation with TNF-α for ALIX, TSG101, CD9, eNOS, VCAM-1, ATP5A, and Histone H3. sEND1 cell pellets, EV-depleted cell culture supernatants (EV-dep), and cell culture media that was not exposed to cells (control) were used as controls. EC-EV miRNA levels of (*G*) hsa-miRNA-126-3p and (*H*) hsa-miRNA-126-5p under basal conditions ($n = 8$) and after inflammatory stimulation with TNF-α ($n = 7$). An unpaired *t*-test was used in (*A*), (*B*), (*C*), (*G*), and (*H*) for statistical analysis. Error bars represent mean ± SD $^{**}P < 0.01$, $^{***}P < 0.001$.

EC-EV localization in the spleen would alter gene expression within spleen tissue, with a focus on CXC chemokine and cytokine activity.

EC-EVs significantly induced mRNA expression for *Cxcr2, Itag4, Gapdh* (all, $P < 0.05$), *Il-1β, Cxcl1* (both, $P < 0.01$), *Cxcr4*, and *Il-6* (both, $P < 0.001$) post-EC-EV injection (*Figure 6B*).

We further determined whether delivery of EC-EVs to the spleen altered chemokine protein levels, including for the retention chemokine CXCL12/SDF-1. In the same mice, we undertook the quantitative protein-detection array for 25 different proteins that influence neutrophil function, including CXCL12/SDF-1, CCL2,[38] and CCL3,[39] which are known miRNA-126-mRNA targets and CCL27/CCL28, which are predicted miRNA-126-mRNA targets. There were significant reductions in CCL21 ($P < 0.01$), CXCL13 ($P < 0.05$), chemerin/retinoic acid receptor responder protein 2 ($P < 0.01$), IL-16 ($P < 0.05$), MCP-5/CCL12 ($P < 0.05$), and CXCL12/SDF-1 ($P < 0.05$) (*Figure 6C*). These findings are consistent with a role for EC-EV-miRNA-126 in silencing genes involved in cell retention.

3.11 EC-EVs mobilize neutrophils from the spleen

Given the effects of the EC-EVs derived from TNF-α activated cells on gene expression and silencing of retention chemokines, we injected EC-

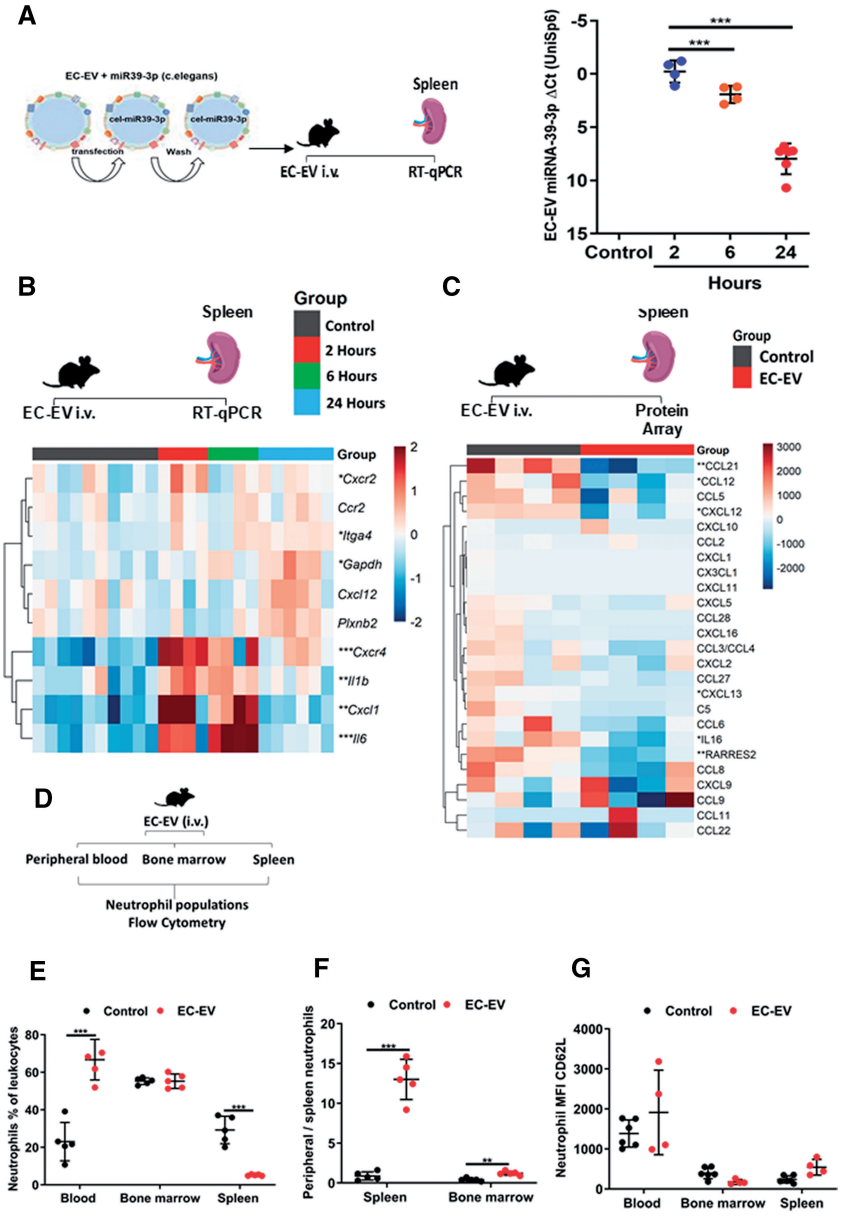

Figure 6 Mouse EC-EVs localize to the spleen in WT mice and influence gene and protein expression and mobilize splenic-neutrophils. (*A*) RT–qPCR detection of EC-EV labelled with miRNA-39-3p in the spleen of mice following intravenous injection of 1×10^9 EVs by tail vein at: 2 ($n = 4$) and 6 h ($n = 4$) post-injection and control injections ($n = 5$); and 24 h ($n = 6$) post-injection and control injections ($n = 5$). Control represents a media only preparation with no EC-EVs. (*B*) Heat map showing gene expression in the spleen of mice following intravenous injection of 1×10^9 EVs by tail vein at 2 ($n = 4$) and 6 h ($n = 4$) post-injection and control injections ($n = 5$); and 24 h ($n = 6$) post-injection and control injections ($n = 5$). Control represents a media only preparation with no EC-EVs. Data shown as ΔΔCt values normalized to row mean ΔΔCt value for each gene. (*C*) Heat map showing protein expression in the spleen of mice following intravenous injection of 1×10^9 EVs by tail vein at 2 h ($n = 4$) post-injection. Control ($n = 4$) represents a media only preparation with no EC-EVs. Data shown are chemokine array dot blot density values normalized to mean row value for each protein. (*D*) Schematic of experiment. (*E*) Percentage of neutrophils as a proportion of the total leukocytes (live, $CD45^+$, $CD11b^+$, and $Ly6G^+$) in peripheral blood, bone marrow, and spleen ($n = 5$ per group). (*F*) Splenic-neutrophil mobilization ratio (peripheral blood neutrophils/spleen neutrophils) shows net contributions of neutrophil reserves to mobilized peripheral blood neutrophils following intravenous injections of EC-EV (1×10^9 EVs/mL) injections ($n = 5$ per group). (*G*) Mean fluorescent intensity of CD62L/L-selectin on neutrophils in peripheral blood, spleen, and bone marrow 2 h after ($n = 5$ per group) intravenous injections of EC-EV (1×10^9 EVs/mL). A one-way ANOVA with *post-hoc* Bonferroni correction was used in (*A*), (*B*), and an unpaired *t*-test was used in (*C*). An unpaired *t*-test was used in (*E*)–(G). Error bars represent mean ± SD $^*P < 0.05$, $^{**}P < 0.01$, $^{***}P < 0.001$.

EVs, derived from TNF-α activated ECs, intravenously into healthy WT mice vs. control media only injections with no EC-EVs (*Figure 6D*). Flow cytometry (Live, $CD45^+$, $CD11b^+$, $Ly6G^+$) showed that EC-EVs significantly increased the number of circulating peripheral blood neutrophils (*Figure 6E*), and simultaneously lowered splenic-neutrophil numbers in the same mice (*Figure 6F*), confirming splenic-neutrophil mobilization induced by EC-EV. Consistent with our observations in AMI, we found that EC-EVs mediated greater neutrophil mobilization from the spleen ($P < 0.001$) than from the bone marrow (*Figure 6F*). As in the context of AMI, there was no alteration in CD62L/L-selectin expression in blood neutrophils (*Figure 6G*).

3.12 EC-EV-VCAM-1 mediates neutrophil mobilization

VCAM-1 positive EVs increases in the immediate hours after AMI (*Figure 2G*). Similarly, ECs in culture produce EVs enriched for VCAM-1 following pro-inflammatory stimulation (*Figure 5E*). Given its well-established role in mediating interactions between activated vascular endothelium and circulating leukocytes, we hypothesized that VCAM-1 on the surface of EC-EVs might perform the converse role by mediating the capture of circulating EC-EVs by static neutrophils in the spleen. We confirmed the presence of VCAM-1 on the surface of plasma EVs using immunoaffinity capture. Magnetic beads of iron oxide were conjugated to IgG control or anti-VCAM-1 antibodies and incubated with isolated human plasma EVs. Subsequent TEM shows specific capture of VCAM-1+ plasma EVs from a heterogenous pool through EV-surface expression of VCAM-1 (*Figure 7A* and Supplementary material online, *Figures S6A–E and S7A–F*).

We next used CRISPR-Cas9 base editing of ECs to produce VCAM-1 deficient EC-EVs by introducing a stop codon in the VCAM-1 sequence. To confirm CRISPR-Cas9 editing of VCAM-1 from ECs, we stimulated WT and VCAM-1 knock-out (KO) cells with TNF-α. WT mouse ECs expressed more VCAM-1 following inflammatory stimulation ($P < 0.001$) (*Figure 7B and C*), whereas VCAM-1 KO cells did not express VCAM-1, confirming successful CRISPR-Cas9 base editing in ECs. VCAM-1 KO cells released EC-EV under basal conditions similar to WT cells (*Figure 7D and E*) but VCAM-1 KO ECs did not release more EVs following inflammatory stimulation with TNF-α (*Figure 7D and E*). WT and VCAM-1 KO EC-EV were positive for EV-markers TSG101 and CD9 but only WT inflammatory-derived EC-EVs were positive for VCAM-1 (*Figure 7F*). EC-EVs derived from either TNF-α-activated WT or TNF-α-activated VCAM-1 KO cells were injected into healthy, WT mice at the same concentration (1×10^9/mL EC-EVs). Using the miRNA-39-3p labelling technique (described above), we found that VCAM-1 deficient EC-EVs and WT EC-EV accumulate in the spleen at similar levels (*Figure 7G*), but VCAM-1 deficient EC-EVs did not induce alteration in gene expression that were comparable to WT EC-EVs responses in the spleen for *Il-6* ($P < 0.001$), *Il-1β* ($P < 0.05$), and *Cxcl1* ($P < 0.05$) (*Figure 7J*). Deletion of VCAM-1 in EC-EVs prevented mobilization of splenic-neutrophils to peripheral blood when compared to WT VCAM-1+ EC-EVs (*Figure 7I and J*).

4. Discussion

Mobilization of neutrophils occurs rapidly after AMI in mice and humans[1,3,4] and their number in peripheral blood correlates with the extent of myocardial injury.[1–3] The bone marrow has been regarded as the principal source for neutrophils that are mobilized to peripheral blood after injury, because (i) it is the primary site for granulopoiesis;[8–10] (ii) it contains ample reserves of mature cells; and (iii) releases neutrophils in response to injection of exogenous chemokines.[12–16] However, the divergent timings of neutrophil mobilization (rapid)[1,7] and chemokine elevation (delayed) *in vivo*[17,18,40] suggest that additional processes may be involved.

Here, we have identified a previously unknown mechanism by which ischaemic injury to the myocardium signals to mobilization of neutrophils from a splenic reserve. We show that: (i) EC-EV generated under conditions of inflammation are enriched for VCAM-1, miRNA-126-3p, and miRNA-126-5p and are elevated in peripheral blood at presentation; (ii) EC-EVs are delivered to the spleen, where they alter gene and protein expression; and (iii) induce the mobilization of splenic-neutrophils to peripheral blood. Notably, (iv) these EC-EV effects are dependent on VCAM-1. Furthermore, (v) we show that neutrophil transcriptomes are differentially regulated following AMI, prior to entry into the myocardium. (vi) Targets of miRNA-126 are significantly altered in neutrophil transcriptomes post-AMI and (vii) administration of miRNA-126 antagomir significantly reduces infarct size *in vivo*.

We utilized a systemic antagomiR strategy to determine the influence of miRNA-126 on infarct size in our rodent model. Treatment of mice by intraperitoneal injection with an antagomiR by repeated injections 5 and 2 days prior to AMI surgery may result in off target effects and does not selectively interfere with neutrophil mobilization from the spleen. However, the data reported here are consistent with a role for miRNA-126 in neutrophil activation and show lower cardiac injury following antagomiR treatment, possibly through abrogated neutrophil activation or recruitment to the injured heart. Future investigations into the role of miRNA-126 in neutrophil activation in the rodent model of AMI may benefit from more selective targeting of neutrophils through genetic approaches or the use of bioengineered EC-EV for specific immunomodulation.

Mature neutrophils are held in large numbers in the haemopoietic cords through interactions with the neutrophil receptors CXCR2 and CXCR4.[11,41,42] Loss of CXCL12 induces an increase in peripheral blood neutrophils. Injection of chemotactic factors,[13] CXCL chemokines,[12,14] and G-CSF[15,16] can drive the rapid mobilization of neutrophils across the sinusoidal endothelium through alterations in CXCR4-CXCL12.

Numerous studies have shown that neutrophil elevation in the blood and myocardium within 24 h in the rodent model of AMI but neutrophils are already elevated in patient blood by the time of arrival at the hospital. Scrutiny of the relative timings of cytokine elevation after ischaemic injury in relation to neutrophil mobilization does not support their role in this early mobilization, since both the onset and peaks in neutrophil mobilization occur prior to those for cytokine elevation.[17,18,40] IL-8 injection mobilized neutrophils from the bone marrow,[13] but after reperfusion in AMI, even in blood from the coronary sinus (undiluted myocardial effluent), the elevation is modest (0.1-fold).[18,19] Furthermore, we calculate that the absolute concentration based on these physiological measurements is ~2–3 orders of magnitude less than the concentration used to elicit neutrophil mobilization in mice.[14] Finally, neutrophils are the first cells to arrive in the acutely injured tissue. Neutrophil depletion dampens plasma chemokines levels following AMI[7] and in a mouse air pouch model.[43] It is not clear which other cells in the profoundly ischaemic myocardium could be capable of the rapid synthesis of chemokines, that would be of sufficient magnitude to mediate neutrophil mobilization from a remote site, such as the bone marrow. The sympathetic nervous system is also activated following AMI and mobilizes committed myeloid lineage cells and neutrophil progenitors from the bone marrow.[44]

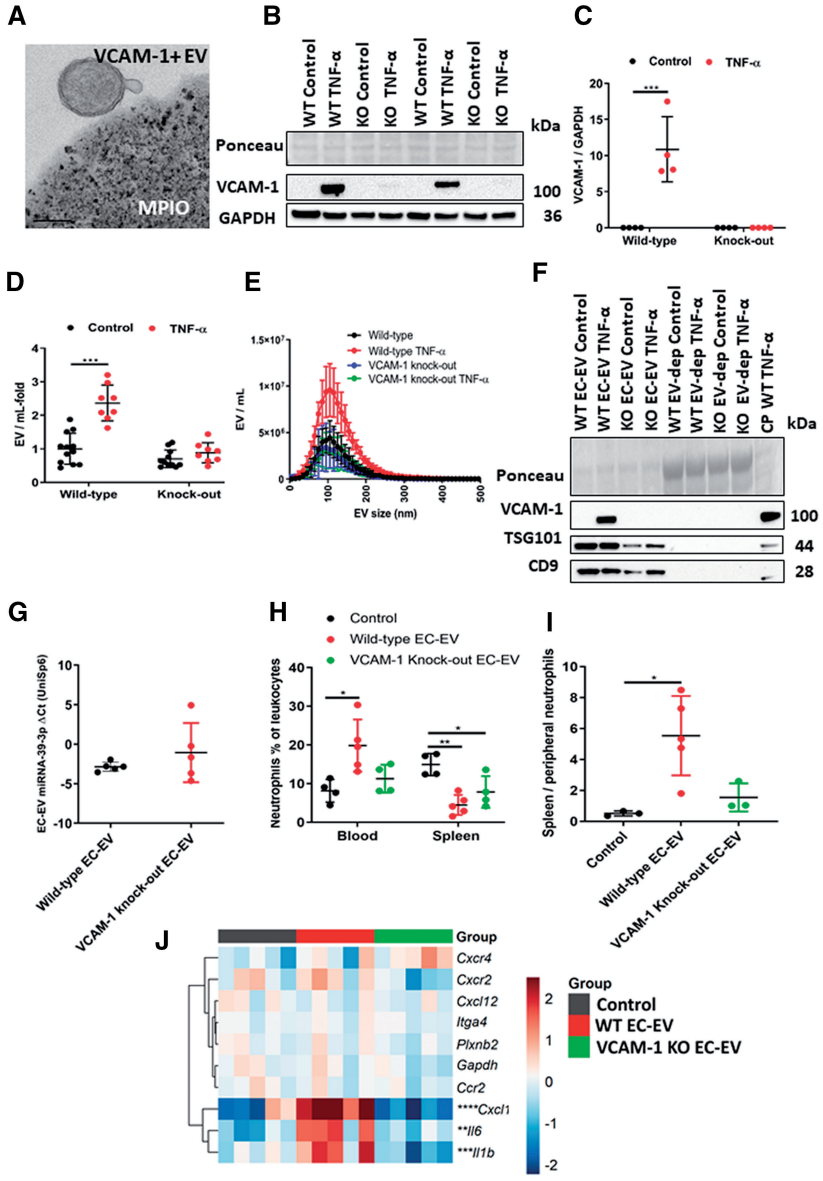

Figure 7 EV VCAM-1 is necessary for EC-EV splenic-neutrophil mobilization in mice. (*A*) TEM of a VCAM-1+ plasma EV bound to a magnetic bead of iron oxide conjugated with anti-human VCAM-1 antibodies, scale bar is 200 nm. (*B*/*C*) Western blot of sEND.1 WT and CRISPR-cas9 base-edited VCAM-1 KO cell pellets under basal conditions (WT $n = 4$ and VCAM-1 KO $n = 4$ per group) and after inflammatory stimulation with recombinant mouse tumour necrosis (TNF-α). (*D*) The number of mouse sEND.1 EC-EVs from WT and CRISPR-cas9 base-edited VCAM-1 KOs under basal conditions (WT $n = 12$ and VCAM-1 KO $n = 11$ per group) and after inflammatory stimulation with recombinant mouse TNF-α ($n = 8$ per group). (*E*) Size and concentration profile of mouse sEND.1 EC-EVs from WT and CRISPR/Cas9 base-edited VCAM-1 KOs under basal conditions (WT $n = 12$ and VCAM-1 KO $n = 11$ per group) and after inflammatory stimulation with recombinant mouse TNF-α ($n = 8$ per group). (*F*) Ponceau stain and western blot of WT and CRISPR-case9 base-edited VCAM-1 KO sEND.1-derived EVs from basal and after inflammatory stimulation with recombinant mouse TNF-α for TSG101, CD9, and VCAM-1. Inflammatory stimulated sEND1 cell pellets and EV-depleted cell culture supernatants were used as controls. (*G*) RT–qPCR detection of WT sEND.1 and CRISPR-cas9 base-edited VCAM-1 KOs EC-EV labelled with miRNA-39-3p in the spleen of mice following intravenous injection of 1×10^9 EVs by tail vein at 2 h post-injection ($n = 5$ per group). (*H*/*I*) Percentage of neutrophils as a proportion of the total leukocytes (live, $CD45^+$, $CD11b^+$, and $Ly6G^+$) in peripheral blood and spleen (control and VCAM-1 KO EC-EV $n = 4$ and WT EC-EV $n = 5$ per group). (*I*) Splenic-neutrophil mobilization ratio (peripheral blood neutrophils/spleen neutrophils) shows net contributions of splenic reserves to mobilized peripheral blood neutrophils following intravenous injections of WT or CRISPR-cas9 base-edited VCAM-1 KO EC-EVs 1×10^9 EVs by tail vein at 2 h post-injection. Control represents a media only preparation with no EC-EVs (control and VCAM-1 KO EC-EV $n = 3$ and WT EC-EV $n = 5$ per group). (*J*) Heat map showing mRNA expression in the spleen of mice following intravenous injection of WT or CRISPR-cas9 base-edited VCAM-1 KO EC-EVs 1×10^9 EVs by tail vein at 2 h post-injection. Control represents a media only preparation with no EC-EVs ($n = 5$ per group). Data shown as ΔΔCt values normalized to row mean ΔΔCt value for each gene. One-way (*H–J*) and two-way (*B–E*) ANOVA with *post-hoc* Bonferroni correction was used for statistical analysis. An unpaired *t*-test was used in (*F*). Error bars represent mean ± SD $^*P < 0.05$, $^{**}P < 0.01$, $^{***}P < 0.001$, $^{****}P < 0.0001$.

However, unlike terminally differentiated neutrophils, blood numbers of myeloid lineage committed cells and neutrophil progenitors do not peak until >6 h post-AMI, subsequent to the increase in peripheral blood neutrophils.

By contrast, numerous studies have shown that hypoxia promotes the rapid (<30 min) release of EVs by ECs.[37] We show that activated ECs in culture liberate large amounts of EV that contain VCAM-1 in their membranes. Using CRISPR/Cas9 genome base editing of cultured ECs, we generated VCAM-1-deficient EV and showed that while VCAM-1 was not essential for splenic localization, its absence removed the ability of EV to provoke the rapid mobilization of neutrophils. Importantly, EVs are taken up rapidly and selectively by the spleen where they become locally concentrated,[23,45] unlike chemokines, which have a systemic effect.

Following injury to the myocardium there is a marked increase in VCAM-1-bearing EVs. VCAM-1 is a glycoprotein, which is expressed on activated endothelium and has a well-established role in the recruitment of circulating leukocytes by binding integrins,[30,46,47] including CD49d.[48] Therefore, our findings suggest an efficient signalling system, in which neutrophils are activated and mobilized by engaging VCAM-1-bearing EVs that are taken up in the spleen, having been released remotely from activated endothelium. A subsequent interaction between neutrophils in circulation and static VCAM-1 on activated ECs mediates their recruitment to the original site of injury.

Deficiency of VCAM-1 by CRISPR/Cas9 in ECs impaired EC-EV release following TNF-α stimulation. The underlying mechanism for this remains unknown, but cellular integrins, such as MAC-1 form important signalling pathways for EV biogenesis in neutrophils[49] and similarly, VCAM-1 may be necessary for inflammation induced EC-EV biogenesis.

The recruitment of neutrophils to the injured myocardium is an essential step in tissue response to injury and repair[1,7] and thus modulating the neutrophil response raises possibilities for immuno-modulatory interventions in selected inflammatory pathologies, including AMI. Peripheral blood neutrophils are elevated at time of presentation with AMI in patients and rapidly increase in peripheral blood following AMI in mice. Here, we show that splenic-neutrophils are rapidly mobilized to peripheral blood by EC-EV-bearing VCAM-1. These findings complement the current paradigm in which neutrophils are liberated from bone marrow reserves through elevations in blood chemokines. We demonstrate a novel and efficient signalling mechanism between the injured heart microvasculature and the spleen. ECs are ideally placed for the rapid release of EVs to peripheral blood during ischaemia. EV clearance is rapid and predominately to the spleen, which contains neutrophils in the supcapsular red pulp. Precisely how neutrophils are retained in the spleen is not known, but our findings suggest that local chemokine signalling may be important, as delivery of EC-EVs rich in miRNA-126 down-regulates retention chemokines, including the miRNA-126 target CXCL12, and induces expression of neutrophil mobilization signals, namely CXCL1.

Importantly, we show that these processes are dependent on EV-VCAM-1, an integrin ligand with a well-documented role in immune cell recruitment. Furthermore, we make a new observation that peripheral blood neutrophils are transcriptionally activated prior to recruitment to the injured myocardium, with a bias towards miRNA-126-mRNA targets. Our bioinformatics analysis revealed SRP-dependent co-translational protein targeting to membrane as the most significantly enriched pathway that was conserved between the human and the mouse blood neutrophils following AMI. SRP is necessary for transferring newly synthesized nascent proteins from the ribosome, which are destined for cellular excretion. Enrichment of SRP-dependent pathways prior to tissue recruitment may prime neutrophils for subsequent degranulation and protein secretion. At 1 day post-AMI neutrophils in the myocardium display significant enrichment for degranulation and protein secretion.[50] A significant enrichment for the universally conserved SRP supports our conclusion that neutrophils are transcriptionally active prior to recruitment to the injured heart. Targeting SRP may open novel opportunities to target neutrophils prior to tissue recruitment to modulate their survival and function, thereby protecting injured tissues from pro-inflammatory neutrophil mediated damage.

In conclusion, we demonstrate that the injured myocardium can rapidly mobilize splenic-neutrophils through generation and release of EC-EVs that bear VCAM-1. These findings provide novel insights into how neutrophils are mobilized to peripheral blood following ischaemic injury, without the need for immediate generation and release of chemokines. EVs are decorated in surface proteins and integrins, which allows them to interact with cells and home to specific sites.[51,52] A functionally efficient reciprocity may operate, in which VCAM-1 on EC-EVs is required for the mobilization of splenic-neutrophils, complementing the known role of static VCAM-1 in the recruitment of circulating neutrophils to activated endothelium. Neutrophils are the first cells recruited to the ischaemic myocardium and are a major source of chemokines.[7] Thus, the well-established mobilization of neutrophils from bone marrow reserves in response to chemokines[12–16] represent a secondary response, which is consistent with the time course of earlier reports and with our observations that there is no rapid bone marrow mobilization in the early phase.

We have shown proof of concept that genetic manipulation can alter EV properties in functionally important ways. Immunomodulation of the neutrophil and monocyte response to AMI using EV vectors may provide therapeutic opportunities in AMI.

Supplementary material

Supplementary material is available at *Cardiovascular Research* online.

Acknowledgements

The authors thank the staff at the Oxford Heart Centre for the clinical care of patients recruited in the coordination of the OxAMI study. Phil Townsend and Steve Woodhouse are gratefully acknowledged for general laboratory management. The authors thank biomedical services staff for their expert care of mice used in this study. The OxAMI study is supported by the British Heart Foundation (BHF; grant CH/16/1/32013 to K.M.C.), the BHF Centre of Research Excellence, Oxford (RG/13/1/30181), the National Institute for Health Research Biomedical Research Centre, Oxford, and the Biomedical Sequencing Facility (BSF) at CeMM for assistance with next-generation sequencing. See Supplementary Acknowledgements online for OxAMI details.

Authors' contributions

N.A. isolated, characterized, and utilized EVs in the described experiments and performed western blots, RT–qPCR, chemokine arrays, analysis of infarcted hearts, and assisted with *in silico* bioinformatics. A.T.B., C.L., D.P., E.L., L.E., G.E.M., E.M.C., and C.v.S. assisted with experimentation. E.M.C., G.J.K., and C.v.S. undertook antagomiR experiments. R.B. and M.M.J. undertook the EV-array. A.T.B. performed bioinformatics analysis and generated transcriptome analysis graphs and heat maps.

A.L.C. and D.P. prepared and analysed flow cytometry preparations. A.C., R.D. and E.J. imaged EVs by TEM/Cryo-TEM. M.G.H. performed some AMI surgeries. T.K. and C.B. performed RNA sequencing. J.R. performed CRISPR-cas9 base editing of endothelial cells. K.J.M., P.R., K.M., and D.A. led animal investigations. R.P.C. and K.M.C. led human AMI investigations. N.A. and R.P.C. conceived the study. All authors participated in study design, coordination, and helped to draft the manuscript. All authors have seen the final version of the manuscript and approve of its submission.

Funding

This work was supported by research grants from the British Heart Foundation (BHF) Centre of Research Excellence, Oxford (N.A. and R.P.C.: RE/13/1/30181 and RE/18/3/34214); British Heart Foundation Project Grant (N.A. and R.P.C.: PG/18/53/33895); the Tripartite Immunometabolism Consortium, Novo Nordisk Foundation (R.P.C.: NNF15CC0018486); Oxford Biomedical Research Centre (BRC); Nuffield Benefaction for Medicine and the Wellcome Institutional Strategic Support Fund (ISSF) (N.A.); the National Institutes of Health (NIHR) [R35HL135799, P01HL131478 (K.J.M.) and T32HL098129 (C.v.S.)]; the American Heart Association [19CDA346300066 (C.v.S.)] and D.R.F.C. and G.E.M. acknowledge Biotechnology and Biological Sciences Research Council (BB/P006205/1).

Conflict of interest: none declared.

Data availability statement

RNA-Sequencing data are deposited at Gene Expression Omnibus (GSE187571) and available by contacting the corresponding author. The data underlying this article are available in Gene Expression Omnibus at https://www.ncbi.nlm.nih.gov/geo/, and can be accessed with GSE187571 and upon reasonable request to the corresponding author.

References

1. Schloss MJ, Horckmans M, Nitz K, Duchene J, Drechsler M, Bidzhekov K, Scheiermann C, Weber C, Soehnlein O, Steffens S. The time-of-day of myocardial infarction onset affects healing through oscillations in cardiac neutrophil recruitment. *EMBO Mol Med* 2016;**8**:937–948.
2. Guo T-M, Cheng B, Ke L, Guan S-M, Qi B-L, Li W-Z, Yang B. Prognostic value of neutrophil to lymphocyte ratio for in-hospital mortality in elderly patients with acute myocardial infarction. *Curr Med Sci* 2018;**38**:354–359.
3. Kong T, Kim TH, Park YS, Chung SP, Lee HS, Hong JH, Lee JW, You JS, Park I. Usefulness of the delta neutrophil index to predict 30-day mortality in patients with ST segment elevation myocardial infarction. *Sci Rep* 2017;**7**:15718.
4. Sreejit G, Abdel-Latif A, Athmanathan B, Annabathula R, Dhyani A, Noothi SK, Quaife-Ryan GA, Al-Sharea A, Pernes G, Dragoljevic D, Lal H, Schroder K, Hanaoka BY, Raman C, Grant MB, Hudson JE, Smyth SS, Porrello ER, Murphy AJ, Nagareddy PR. Neutrophil-derived S100A8/A9 amplify granulopoiesis after myocardial infarction. *Circulation* 2020;**141**:1080–1094.
5. Chia S, Nagurney JT, Brown DFM, Raffel OC, Bamberg F, Senatore F, Wackers FJT, Jang I-K. Association of leukocyte and neutrophil counts with infarct size, left ventricular function and outcomes after percutaneous coronary intervention for ST-elevation myocardial infarction. *Am J Cardiol* 2009;**103**:333–337.
6. Lörchner H, Pöling J, Gajawada P, Hou Y, Polyakova V, Kostin S, Adrian-Segarra JM, Boettger T, Wietelmann A, Warnecke H, Richter M, Kubin T, Braun T. Myocardial healing requires Reg3beta-dependent accumulation of macrophages in the ischemic heart. *Nat Med* 2015;**21**:353–362.
7. Horckmans M, Ring L, Duchene J, Santovito D, Schloss MJ, Drechsler M, Weber C, Soehnlein O, Steffens S. Neutrophils orchestrate post-myocardial infarction healing by polarizing macrophages towards a reparative phenotype. *Eur Heart J* 2017;**38**:187–197.
8. Evrard M, Kwok IWH, Chong SZ, Teng KWW, Becht E, Chen J, Sieow JL, Penny HL, Ching GC, Devi S, Adrover JM, Li JLY, Liong KH, Tan L, Poon Z, Foo S, Chua JW, Su IH, Balabanian K, Bachelerie F, Biswas SK, Larbi A, Hwang WYK, Madan V, Koeffler HP, Wong SC, Newell EW, Hidalgo A, Ginhoux F, Ng LG. Developmental analysis of bone marrow neutrophils reveals populations specialized in expansion, trafficking, and effector functions. *Immunity* 2018;**48**:364–379.e368.
9. Zhu YP, Padgett L, Dinh HQ, Marcovecchio P, Blatchley A, Wu R, Ehinger E, Kim C, Mikulski Z, Seumois G, Madrigal A, Vijayanand P, Hedrick CC. Identification of an early unipotent neutrophil progenitor with pro-tumoral activity in mouse and human bone marrow. *Cell Rep* 2018;**24**:2329–2341.e2328.
10. Horckmans M, Bianchini M, Santovito D, Megens RTA, Springael J-Y, Negri I, Vacca M, Di Eusanio M, Moschetta A, Weber C, Duchene J, Steffens S. Pericardial adipose tissue regulates granulopoiesis, fibrosis, and cardiac function after myocardial infarction. *Circulation* 2018;**137**:948–960.
11. Furze RC, Rankin SM. Neutrophil mobilization and clearance in the bone marrow. *Immunology* 2008;**125**:281–288.
12. Martin C, Burdon PCE, Bridger G, Gutierrez-Ramos JC, Williams TJ, Rankin SM. Chemokines acting via CXCR2 and CXCR4 control the release of neutrophils from the bone marrow and their return following senescence. *Immunity* 2003;**19**:583–593.
13. Terashima T, English D, Hogg JC, van Eeden SF. Release of polymorphonuclear leukocytes from the bone marrow by interleukin-8. *Blood* 1998;**92**:1062–1069.
14. Jagels MA, Hugli TE. Neutrophil chemotactic factors promote leukocytosis. A common mechanism for cellular recruitment from bone marrow. *J Immunol* 1992;**148**:1119–1128.
15. Semerad CL, Liu FL, Gregory AD, Stumpf K, Link DC. G-CSF is an essential regulator of neutrophil trafficking from the bone marrow to the blood. *Immunity* 2002;**17**:413–423.
16. Köhler A, De Filippo K, Hasenberg M, van den Brandt C, Nye E, Hosking MP, Lane TE, Männ L, Ransohoff RM, Hauser AE, Winter O, Schraven B, Geiger H, Hogg N, Gunzer M. G-CSF-mediated thrombopoietin release triggers neutrophil motility and mobilization from bone marrow via induction of Cxcr2 ligands. *Blood* 2011;**117**:4349–4357.
17. Deten A, Volz HC, Briest W, Zimmer HG. Cardiac cytokine expression is upregulated in the acute phase after myocardial infarction. Experimental studies in rats. *Cardiovasc Res* 2002;**55**:329–340.
18. Neumann F-J, Ott I, Gawaz M, Richardt G, Holzapfel H, Jochum M, SchöMig A. Cardiac release of cytokines and inflammatory responses in acute myocardial infarction. *Circulation* 1995;**92**:748–755.
19. Marx N, Neumann FJ, Ott I, Gawaz M, Koch W, Pinkau T, Schömig A. Induction of cytokine expression in leukocytes in acute myocardial infarction. *J Am Coll Cardiol* 1997;**30**:165–170.
20. Puga I, Cols M, Barra CM, He B, Cassis L, Gentile M, Comerma L, Chorny A, Shan M, Xu W, Magri G, Knowles DM, Tam W, Chiu A, Bussel JB, Serrano S, Lorente JA, Bellosillo B, Lloreta J, Juanpere N, Alameda F, Baró T, de Heredia CD, Torán N, Català A, Torrebadell M, Fortuny C, Cusí V, Carreras C, Diaz GA, Blander JM, Farber C-M, Silvestri G, Cunningham-Rundles C, Calvillo M, Dufour C, Notarangelo LD, Lougaris V, Plebani A, Casanova J-L, Ganal SC, Diefenbach A, Aróstegui JI, Juan M, Yagüe J, Mahlaoui N, Donadieu J, Chen K, Cerutti A. B cell-helper neutrophils stimulate the diversification and production of immunoglobulin in the marginal zone of the spleen. *Nat Immunol* 2011;**13**:170–180.
21. Deniset JF, Surewaard BG, Lee WY, Kubes P. Splenic Ly6G(high) mature and Ly6G(int) immature neutrophils contribute to eradication of S. pneumoniae. *J Exp Med* 2017;**214**:1333–1350.
22. Swirski FK, Nahrendorf M, Etzrodt M, Wildgruber M, Cortez-Retamozo V, Panizzi P, Figueiredo J-L, Kohler RH, Chudnovskiy A, Waterman P, Aikawa E, Mempel TR, Libby P, Weissleder R, Pittet MJ. Identification of splenic reservoir monocytes and their deployment to inflammatory sites. *Science* 2009;**325**:612–616.
23. Akbar N, Digby JE, Cahill TJ, Tavare AN, Corbin AL, Saluja S, Dawkins S, Edgar L, Rawlings N, Ziberna K, McNeill E; Oxford Acute Myocardial Infarction (OxAMI) Study, Johnson E, Aljabali AA, Dragovic RA, Rohling M, Belgard TG, Udalova IA, Greaves DR, Channon KM, Riley PR, Anthony DC, Choudhury RP. Endothelium-derived extracellular vesicles promote splenic monocyte mobilization in myocardial infarction. *JCI Insight* 2017;**2**:e93344.
24. Thery C, Witwer KW, Aikawa E, Alcaraz MJ, Anderson JD, Andriantsitohaina R, Antoniou A, Arab T, Archer F, Atkin-Smith GK, Ayre DC, Bach JM, Bachurski D, Baharvand H, Balaj L, Baldacchino S, Bauer NN, Baxter AA, Bebawy M, Beckham C, Bedina Zavec A, Benmoussa A, Berardi AC, Bergese P, Bielska E, Blenkiron C, Bobis-Wozowicz S, Boilard E, Boireau W, Bongiovanni A, Borràs FE, Bosch S, Boulanger CM, Breakefield X, Breglio AM, Brennan MÁ, Brigstock DR, Brisson A, Broekman ML, Bromberg JF, Bryl-Górecka P, Buch S, Buck AH, Burger D, Busatto S, Buschmann D, Bussolati B, Buzás EI, Byrd JB, Camussi G, Carter DR, Caruso S, Chamley LW, Chang YT, Chen C, Chen S, Cheng L, Chin AR, Clayton A, Clerici SP, Cocks A, Cocucci E, Coffey RJ, Cordeiro-da-Silva A, Couch Y, Coumans FA, Coyle B, Crescitelli R, Criado MF, D'Souza-Schorey C, Das S, Datta Chaudhuri A, de Candia P, De Santana EF, De Wever O, Del Portillo HA, Demaret T, Deville S, Devitt A, Dhondt B, Di Vizio D, Dieterich LC, Dolo V, Dominguez Rubio AP, Dominici M, Dourado MR, Driedonks TA, Duarte FV, Duncan HM, Eichenberger RM, Ekström K, El Andaloussi S, Elie-Caille C, Erdbrügger U, Falcón-Pérez JM, Fatima F, Fish JE, Flores-Bellver M, Försönits A, Frelet-Barrand A, Fricke F, Fuhrmann G, Gabrielsson S, Gámez-Valero A, Gardiner C, Gärtner K, Gaudin R, Gho YS, Giebel B, Gilbert C, Gimona M, Giusti I, Goberdhan DC, Görgens A, Gorski SM, Greening DW, Gross JC, Gualerzi A, Gupta GN, Gustafson D, Handberg A, Haraszti RA, Harrison P, Hegyesi H, Hendrix A, Hill AF, Hochberg FH, Hoffmann KF, Holder B, Holthofer H, Hosseinkhani B, Hu G, Huang Y, Huber V, Hunt S, Ibrahim AG, Ikezu T, Inal JM, Isin M, Ivanova A, Jackson HK, Jacobsen S, Jay SM, Jayachandran M, Jenster G, Jiang L, Johnson SM, Jones JC, Jong A, Jovanovic-Talisman T, Jung S, Kalluri R, Kano SI, Kaur S, Kawamura Y, Keller ET, Khamari D, Khomyakova E, Khvorova A, Kierulf P, Kim KP,

Kislinger T, Klingeborn M, Klinke DJ 2nd, Kornek M, Kosanović MM, Kovács ÁF, Krämer-Albers EM, Krasemann S, Krause M, Kurochkin IV, Kusuma GD, Kuypers S, Laitinen S, Langevin SM, Languino LR, Lannigan J, Lässer C, Laurent LC, Lavieu G, Lázaro-Ibáñez E, Le Lay S, Lee MS, Lee YXF, Lemos DS, Lenassi M, Leszczynska A, Li IT, Liao K, Libregts SF, Ligeti E, Lim R, Lim SK, Linē A, Linnemannstöns K, Llorente A, Lombard CA, Lorenowicz MJ, Lörincz ÁM, Lötvall J, Lovett J, Lowry MC, Loyer X, Lu Q, Lukomska B, Lunavat TR, Maas SL, Malhi H, Marcilla A, Mariani J, Mariscal J, Martens-Uzunova ES, Martin-Jaular L, Martinez MC, Martins VR, Mathieu M, Mathivanan S, Maugeri M, McGinnis LK, McVey MJ, Meckes DG Jr, Meehan KL, Mertens I, Minciacchi VR, Möller A, Møller Jørgensen M, Morales-Kastresana A, Morhayim J, Mullier F, Muraca M, Musante L, Mussack V, Muth DC, Myburgh KH, Najrana T, Nawaz M, Nazarenko I, Nejsum P, Neri C, Neri T, Nieuwland R, Nimrichter L, Nolan JP, Nolte-'t Hoen EN, Noren Hooten N, O'Driscoll L, O'Grady T, O'Loghlen A, Ochiya T, Olivier M, Ortiz A, Ortiz LA, Osteikoetxea X, Østergaard O, Ostrowski M, Park J, Pegtel DM, Peinado H, Perut F, Pfaffl MW, Phinney DG, Pieters BC, Pink RC, Pisetsky DS, Pogge von Strandmann E, Polakovicova I, Poon IK, Powell BH, Prada I, Pulliam L, Quesenberry P, Radeghieri A, Raffai RL, Raimondo S, Rak J, Ramirez MI, Raposo G, Rayyan MS, Regev-Rudzki N, Ricklefs FL, Robbins PD, Roberts DD, Rodrigues SC, Rohde E, Rome S, Rouschop KM, Rughetti A, Russell AE, Saá P, Sahoo S, Salas-Huenuleo E, Sánchez C, Saugstad JA, Saul MJ, Schiffelers RM, Schneider R, Schøyen TH, Scott A, Shahaj E, Sharma S, Shatnyeva O, Shekari F, Shelke GV, Shetty AK, Shiba K, Siljander PR, Silva AM, Skowronek A, Snyder OL 2nd, Soares RP, Sódar BW, Soekmadji C, Sotillo J, Stahl PD, Stoorvogel W, Stott SL, Strasser EF, Swift S, Tahara H, Tewari M, Timms K, Tiwari S, Tixeira R, Tkach M, Toh WS, Tomasini R, Torrecilhas AC, Tosar JP, Toxavidis V, Urbanelli L, Vader P, van Balkom BW, van der Grein SG, Van Deun J, van Herwijnen MJ, Van Keuren-Jensen K, van Niel G, van Royen ME, van Wijnen AJ, Vasconcelos MH, Vechetti IJ Jr, Veit TD, Vella LJ, Velot É, Verweij FJ, Vestad B, Viñas JL, Visnovitz T, Vukman KV, Wahlgren J, Watson DC, Wauben MH, Weaver A, Webber JP, Weber V, Wehman AM, Weiss DJ, Welsh JA, Wendt S, Wheelock AM, Wiener Z, Witte L, Wolfram J, Xagorari A, Xander P, Xu J, Yan X, Yáñez-Mó M, Yin H, Yuana Y, Zappulli V, Zarubova J, Žėkas V, Zhang JY, Zhao Z, Zheng L, Zheutlin AR, Zickler AM, Zimmermann P, Zivkovic AM, Zocco D, Zuba-Surma EK. Minimal information for studies of extracellular vesicles 2018 (MISEV2018): a position statement of the International Society for Extracellular Vesicles and update of the MISEV2014 guidelines. *J Extracell Vesicles* 2018;**7**:1535750.

25. Akbar N, Azzimato V, Choudhury RP, Aouadi M. Extracellular vesicles in metabolic disease. *Diabetologia* 2019;**62**:2179–2187.
26. Sluijter JPG, Davidson SM, Boulanger CM, Buzás EI, de Kleijn DPV, Engel FB, Giricz Z, Hausenloy DJ, Kishore R, Lecour S, Leor J, Madonna R, Perrino C, Prunier F, Sahoo S, Schiffelers RM, Schulz R, Van Laake LW, Ytrehus K, Ferdinandy P. Extracellular vesicles in diagnostics and therapy of the ischaemic heart: Position Paper from the Working Group on Cellular Biology of the Heart of the European Society of Cardiology. *Cardiovasc Res* 2018;**114**:19–34.
27. Russell AE, Sneider A, Witwer KW, Bergese P, Bhattacharyya SN, Cocks A, Cocucci E, Erdbrügger U, Falcon-Perez JM, Freeman DW, Gallagher TM, Hu S, Huang Y, Jay SM, Kano S-I, Lavieu G, Leszczynska A, Llorente AM, Lu Q, Mahairaki V, Muth DC, Noren Hooten N, Ostrowski M, Prada I, Sahoo S, Schøyen TH, Sheng L, Tesch D, Van Niel G, Vandenbroucke RE, Verweij FJ, Villar AV, Wauben M, Wehman AM, Yin H, Carter DRF, Vader P. Biological membranes in EV biogenesis, stability, uptake, and cargo transfer: an ISEV position paper arising from the ISEV membranes and EVs workshop. *J Extracell Vesicles* 2019;**8**:1684862.
28. Loyer X, Zlatanova I, Devue C, Yin M, Howangyin K-Y, Klaihmon P, Guerin CL, Kheloufi M, Vilar J, Zannis K, Fleischmann BK, Hwang DW, Park J, Lee H, Menasché P, Silvestre J-S, Boulanger CM. Intra-cardiac release of extracellular vesicles shapes inflammation following myocardial infarction. *Circ Res* 2018;**123**:100–106.
29. Cheng M, Yang J, Zhao X, Zhang E, Zeng Q, Yu Y, Yang L, Wu B, Yi G, Mao X, Huang K, Dong N, Xie M, Limdi NA, Prabhu SD, Zhang J, Qin G. Circulating myocardial microRNAs from infarcted hearts are carried in exosomes and mobilise bone marrow progenitor cells. *Nat Commun* 2019;**10**:959.
30. Ross EA, Douglas MR, Wong SH, Ross EJ, Curnow SJ, Nash GB, Rainger E, Scheel-Toellner D, Lord JM, Salmon M, Buckley CD. Interaction between integrin alpha9-beta1 and vascular cell adhesion molecule-1 (VCAM-1) inhibits neutrophil apoptosis. *Blood* 2006;**107**:1178–1183.
31. Jorgensen M, Baek R, Pedersen S, Sondergaard EK, Kristensen SR, Varming K. Extracellular Vesicle (EV) Array: microarray capturing of exosomes and other extracellular vesicles for multiplexed phenotyping. *J Extracell Vesicles* 2013;**2**. Doi: 10.3402/jev.v2i0.20920.
32. Agarwal V, Bell GW, Nam JW, Bartel DP. Predicting effective microRNA target sites in mammalian mRNAs. *Elife* 2015;**4**:e05005.
33. Sticht C, De La Torre C, Parveen A, Gretz N. miRWalk: an online resource for prediction of microRNA binding sites. *PLoS One* 2018;**13**:e0206239.
34. Liu W, Wang X. Prediction of functional microRNA targets by integrative modeling of microRNA binding and target expression data. *Genome Biol* 2019;**20**:18.
35. Jassal B, Matthews L, Viteri G, Gong C, Lorente P, Fabregat A, Sidiropoulos K, Cook J, Gillespie M, Haw R, Loney F, May B, Milacic M, Rothfels K, Sevilla C, Shamovsky V, Shorser S, Varusai T, Weiser J, Wu G, Stein L, Hermjakob H, D'Eustachio P. The reactome pathway knowledgebase. *Nucleic Acids Res* 2020;**48**:D498–D503.
36. Vafadarnejad E, Rizzo G, Krampert L, Arampatzi P, Arias-Loza A-P, Nazzal Y, Rizakou A, Knochenhauer T, Bandi SR, Nugroho VA, Schulz DJJ, Roesch M, Alayrac P, Vilar J, Silvestre J-S, Zernecke A, Saliba A-E, Cochain C. Dynamics of cardiac neutrophil diversity in murine myocardial infarction. *Circ Res* 2020;**127**:e232–e249.
37. Davidson SM, Riquelme JA, Zheng Y, Vicencio JM, Lavandero S, Yellon DM. Endothelial cells release cardioprotective exosomes that may contribute to ischaemic preconditioning. *Sci Rep* 2018;**8**:15885.
38. Arner E, Mejhert N, Kulyté A, Balwierz PJ, Pachkov M, Cormont M, Lorente-Cebrián S, Ehrlund A, Laurencikiene J, Hedén P, Dahlman-Wright K, Tanti J-F, Hayashizaki Y, Rydén M, Dahlman I, van Nimwegen E, Daub CO, Arner P. Adipose tissue microRNAs as regulators of CCL2 production in human obesity. *Diabetes* 2012;**61**:1986–1993.
39. Agudo J, Ruzo A, Tung N, Salmon H, Leboeuf M, Hashimoto D, Becker C, Garrett-Sinha L-A, Baccarini A, Merad M, Brown BD. The miR-126-VEGFR2 axis controls the innate response to pathogen-associated nucleic acids. *Nat Immunol* 2014;**15**:54–62.
40. Rusinkevich V, Huang Y, Chen Z-y, Qiang W, Wang Y-G, Shi Y-F, Yang H-T. Temporal dynamics of immune response following prolonged myocardial ischemia/reperfusion with and without cyclosporine A. *Acta Pharmacol Sin* 2019;**40**:1168–1183.
41. Eash KJ, Means JM, White DW, Link DC. CXCR4 is a key regulator of neutrophil release from the bone marrow under basal and stress granulopoiesis conditions. *Blood* 2009;**113**:4711–4719.
42. Suratt BT, Petty JM, Young SK, Malcolm KC, Lieber JG, Nick JA, Gonzalo J-A, Henson PM, Worthen GS. Role of the CXCR4/SDF-1 chemokine axis in circulating neutrophil homeostasis. *Blood* 2004;**104**:565–571.
43. Garcia-Ramallo E, Marques T, Prats N, Beleta J, Kunkel SL, Godessart N. Resident cell chemokine expression serves as the major mechanism for leukocyte recruitment during local inflammation. *J Immunol* 2002;**169**:6467–6473.
44. Dutta P, Courties G, Wei Y, Leuschner F, Gorbatov R, Robbins CS, Iwamoto Y, Thompson B, Carlson AL, Heidt T, Majmudar MD, Lasitschka F, Etzrodt M, Waterman P, Waring MT, Chicoine AT, van der Laan AM, Niessen HWM, Piek JJ, Rubin BB, Butany J, Stone JR, Katus HA, Murphy SA, Morrow DA, Sabatine MS, Vinegoni C, Moskowitz MA, Pittet MJ, Libby P, Lin CP, Swirski FK, Weissleder R, Nahrendorf M. Myocardial infarction accelerates atherosclerosis. *Nature* 2012;**487**:325–329.
45. Saunderson SC, Dunn AC, Crocker PR, McLellan AD. CD169 mediates the capture of exosomes in spleen and lymph node. *Blood* 2014;**123**:208–216.
46. Forrester JV, Lackie JM. Adhesion of neutrophil leucocytes under conditions of flow. *J Cell Sci* 1984;**70**:93–110.
47. Taooka Y, Chen J, Yednock T, Sheppard D. The integrin alpha9beta1 mediates adhesion to activated endothelial cells and transendothelial neutrophil migration through interaction with vascular cell adhesion molecule-1. *J Cell Biol* 1999;**145**:413–420.
48. Issekutz TB, Miyasaka M, Issekutz AC. Rat blood neutrophils express very late antigen 4 and it mediates migration to arthritic joint and dermal inflammation. *J Exp Med* 1996;**183**:2175–2184.
49. Lőrincz ÁM, Bartos B, Szombath D, Szeifert V, Timár CI, Turiák L, Drahos L, Kittel Á, Veres DS, Kolonics F, Mócsai A, Ligeti E. Role of Mac-1 integrin in generation of extracellular vesicles with antibacterial capacity from neutrophilic granulocytes. *J Extracell Vesicles* 2020;**9**:1698889.
50. Daseke MJ, Valerio FM, Kalusche WJ, Ma Y, DeLeon-Pennell KY, Lindsey ML. Neutrophil proteome shifts over the myocardial infarction time continuum. *Basic Res Cardiol* 2019;**114**:37.
51. Hoshino A, Costa-Silva B, Shen T-L, Rodrigues G, Hashimoto A, Tesic Mark M, Molina H, Kohsaka S, Di Giannatale A, Ceder S, Singh S, Williams C, Soplop N, Uryu K, Pharmer L, King T, Bojmar L, Davies AE, Ararso Y, Zhang T, Zhang H, Hernandez J, Weiss JM, Dumont-Cole VD, Kramer K, Wexler LH, Narendran A, Schwartz GK, Healey JH, Sandstrom P, Labori KJ, Kure EH, Grandgenett PM, Hollingsworth MA, de Sousa M, Kaur S, Jain M, Mallya K, Batra SK, Jarnagin WR, Brady MS, Fodstad O, Muller V, Pantel K, Minn AJ, Bissell MJ, Garcia BA, Kang Y, Rajasekhar VK, Ghajar CM, Matei I, Peinado H, Bromberg J, Lyden D. Tumour exosome integrins determine organotropic metastasis. *Nature* 2015;**527**:329–335.
52. Rodrigues G, Hoshino A, Kenific CM, Matei IR, Steiner L, Freitas D, Kim HS, Oxley PR, Scandariato I, Casanova-Salas I, Dai J, Badwe CR, Gril B, Tešić Mark M, Dill BD, Molina H, Zhang H, Benito-Martin A, Bojmar L, Ararso Y, Offer K, LaPlant Q, Buehring W, Wang H, Jiang X, Lu TM, Liu Y, Sabari JK, Shin SJ, Narula N, Ginter PS, Rajasekhar VK, Healey JH, Meylan E, Costa-Silva B, Wang SE, Rafii S, Altorki NK, Rudin CM, Jones DR, Steeg PS, Peinado H, Ghajar CM, Bromberg J, de Sousa M, Pisapia D, Lyden D. Tumour exosomal CEMIP protein promotes cancer cell colonization in brain metastasis. *Nat Cell Biol* 2019;**21**:1403–1412.

Translational perspective

Peripheral blood neutrophils are rapidly elevated following acute myocardial infarction (AMI) and prior to alterations in systemic cytokines. Extracellular vesicles (EVs) are membrane-enclosed particles that carry protein and miRNAs and are rapidly liberated from endothelial cells (ECs). Here, we show that following AMI EC-derived EVs (EC-EVs) mediate neutrophil mobilization from the spleen via EC-EV-VCAM-1 and induce transcriptional activation of neutrophils in the blood to favour miRNA-126-mRNA targets; miRNA-126 antagomir treatment lowers infarct size. EC-EV-VCAM-1 and EC-EV-miRNA-126 are novel mechanisms that mobilize splenic reserve of neutrophils, a previously unidentified source of neutrophils in sterile ischaemic injury.